A particle model analysing the behavioural rules underlying the collective flight of a bee swarm towards the new nest

(Article begins on next page)

19 April 2024

ARTICLE TEMPLATE

A particle model analyzing the behavioral rules underlying the collective flight of a bee swarm towards the new nest

S. Bernardi, A. Colombi and M. Scianna

Department of Mathematical Sciences, Politecnico di Torino, 10129 Torino, Italy

ABSTRACT
The swarming of a bee colony is guided by a small group of scout individuals, which are informed of the target destination (the new nest). However, little is known on the underlying mechanisms, i.e., on how the information is passed within the population. In this respect, we here present a discrete mathematical model to investigate these aspects. In particular, each bee, represented by a material point, is assigned its status within the colony and set to move according to individual strategies and social interactions. More specifically, we propose alternative assumptions on the flight synchronization mechanism of uninformed individuals and on the characteristic dynamics of the scout insects. Numerical realizations then point out the combinations of behavioral hypotheses resulting in collective productive movement. An analysis of the role of the scout bee percentage and of the phenomenology of the swarm in domains with structural elements is finally performed.

KEYWORDS
bee swarming; alignment mechanisms; coordinate movement; collective animal migration

1. Introduction

The wish of describing emerging *collective* dynamics of populations of interacting individuals, such as birds, fishes, insects and certain mammals, from individual behaviors has increased in the last decades the multidisciplinary interest of various research communities, e.g., biologists, ecologists, sociologists, physicists, and applied mathematicians.

For instance, the coordinated behavior of bee swarms represents an interesting problem to be studied. Such insect populations, which are typically composed by the old queen and by 10000 to 30000 worker individuals, in fact undergo a synchronized flight with the specific purpose of reaching a new nest site [48]. All colonies are subject to this natural phenomenon, and every year beekeepers have to deal with it in late spring and early summer. In this period, as the weather warms up and flowers begin to bloom, the colony is in fact at the peak of its capacity and ready to produce a new hive.

S. Bernardi. Email: sara.bernardi@polito.it

A. Colombi. Email: annachiara.colombi@polito.it

M. Scianna. Email: marco.scianna@polito.it

In this respect, each bee swarm has to face two challenges: it first needs to identify a suitable new location using a process of community site selection and then it has to move towards the chosen destination. Entering in more details, when the migrating bees leave the original hive they first temporarily settle on a tree branch a few meters away from the old nest. There, they cluster around the queen, and a small fraction of bees (called *scouts*) starts exploring the surrounding area. These individuals inspect possible locations for the new nest to assess their quality, in terms of volume, aspect, size and height of entrance, and presence of structures left by other bee colonies [48, 52]. Then, they return to the rest of the population and perform a waggle dance to broadcast information on the characteristics of the explored sites. Nest proposals coming from the scout bees may be different but, after some hours (sometimes days), an agreement is finally found.

The whole swarm finally takes off and compactly flies towards the chosen destination, following the guidance of the informed/scout individuals. In this respect, various assumptions have been proposed to account for the migration mechanisms underlying this leader-follower system. First, it was hypothesized that the scout bees can pilot the cloud of insects to the new home by producing the Nasonov pheromone. However, a subsequent experimental study revealed that such a chemical substance is not really involved in the flight guidance process, while it is crucial to help the uninformed/follower individuals to find the entrance of the new nest [2].

A different family of possible explanations instead involves selected visual signals in the transmission of information within the swarm. Specifically, Lindauer in 1955 proposed that the scout insects can transmit the direction of movement by flying through the swarm [44]. In particular, such informed bees are observed to *streak* at high speed from the back of the swarm to its front. However, once they have reached the front of the cloud, their behavior is still unknown. In this respect, in [46, 48], two possible dynamics are suggested: (i) they may slowly fly back towards the rear edge of the swarm or (ii) they may stop and wait to be passed by the rest of the groupmates. In both cases, the scout bees then start again to streak towards the leading edge of the insect cloud and the process is iterated. The uninformed bees are in turn observed to align their flight towards the position of the new nest. How the follower individuals acquire the information of the correct migration direction under the scout guidance is debated as well. More specifically, each different hypothesis on their flight synchronization mechanism involves the alignment with a distinct set of groupmates, composed, e.g., by faster individuals, or by closer individuals, or only by informed individuals.

1.1. Objective and structure of the work

Our aim is to investigate the individual behavior that is at the basis of bee swarming towards a new nest. In this respect, we will reproduce the dynamics of a bee population with a first-order microscopic discrete model that focuses on the flight phenomenology of each component insect.

In more details, our model will be based on the so-called "first sociological principles of swarming" which state that the individuals forming a flying group are subject at least to repulsive, attractive, and alignment stimuli. These assumptions have been previously implemented in a number of approaches dealing with the collective dynamics of swarms, as commented in the conclusive section of this paper and reviewed by Carrillo and coworkers in [11]. We have also employed such phenomenological rules

in a previous work [3], that has analyzed how a single leader bee is able to transmit the direction of movement to the rest of the population. In particular, we have therein tested alternative alignment hypotheses, i.e., topological vs. metric. The former implies that each insect synchronizes its flight to a given number of groupmates regardless of their effective distance; the latter implies that each bee synchronizes its flight to all groupmates falling within a certain region. The results presented in that work have then demonstrated a directionally efficient swarming can be obtained with a sufficiently large (i.e., with radius equal to the overall extension of the insect cloud) alignment region in the case of metric alignment or with a high enough (i.e., ≥ 13) number of individuals taken into account by each bee in the case of topological alignment. In spite of such interesting results, some aspects characterizing the collective dynamics of bee clouds still remained unexplored, becoming indeed the main focus of this article.

In this respect, we will here first introduce anisotropy in insect behavior by the definition of a more realistic visual region, i.e., not completely round. Then, we will include the experimentally observed bee differentiated behavior within the population: we will in fact distinguish between scout individuals and follower insects and define for each subgroup a specific phenomenology. In particular, we will test different combinations of hypotheses relative (i) to the characteristic movement of the scout/informed bees (which will be indeed described in more details with respect to our previous work, where a single leader individual was set to constantly fly in a given direction) and (ii) to the alignment mechanisms of the follower/uninformed individuals. In more details, each uninformed bee will be assumed to synchronize its movement to a given set of groupmates not only upon considerations on their mutual distance (as in our previous work) but also taking into account their status and actual velocity.

Once the most reasonable assumptions resulting in a correct collective swarming of the insect population is found out, our second objective will be then to demonstrate that the obtained behavioral rules are sufficient to reproduce realistic migratory dynamics in complex real-world scenarios, involving domains with structural elements and obstacles.

The rest of this paper is organized as follows. In Section 2, we will present the main model components. More specifically, we will first explain the characteristic representation of the virtual bees and their possible status/role within the population; then, we will write the equations of motion and introduce the relative velocity contributions. In particular, we will clarify the biological and experimental considerations each term is based on. In Section 3, selected series of numerical realizations will analyze swarm dynamics under different combinations of the proposed behavioral hypotheses of the insect colony. A study on the influence of the fraction of scout individuals on the swarming process will be performed as well. After presenting in Section 3.2 the phenomenology of the bee cloud in more realistic situations, we will review in Section 4 the results obtained in the article. In the same conclusive part of the work, we will compare our approach with similar discrete models dealing with bee dynamics presented in the literature and propose some possible improvements and developments of the work. Finally, Appendix 5 will provide a detailed description of the parameter estimate employed in our theoretical framework.

2. Mathematical model

Bee characteristics and status transitions. A population of bees is modeled in the two-dimensional bounded domain $\Omega \subset \mathbb{R}^2$, whose boundary is defined by $\partial\Omega$. We are indeed considering a planar section, parallel to the ground, of a typical bee swarm, see Fig. 1 (a). We further assume that the new nest, i.e., the target destination of the insects, is constituted by a subregion of the domain boundary, hereafter denoted by $\partial\Omega_{\text{nest}}$ ($\subset \partial\Omega$), refer again to Fig. 1 (a). Each insect $i = 1, ..., N$, being N the total number of individuals, is an autonomous discrete agent, represented by a material point with concentrated mass. In particular, the generic i-th bee is uniquely defined by the following set of variables:

$$(\mathbf{x}_i(t), \mathbf{v}_i(t), \mathbf{g}_i(t), s_i(t)) \in \mathbb{R}^2 \times \mathbb{R}^2 \times S_1^2 \times \mathcal{S}, \tag{1}$$

where S_1^2 is the unit circle. The vectors $\mathbf{x}_i(t)$, $\mathbf{v}_i(t)$, and $\mathbf{g}_i(t)$ denote individual position, velocity, and gazing direction, respectively, whereas $s_i(t)$ is a status variable which defines the role that the insect of interest has within the swarm. In this respect, according to the biological considerations presented in the previous section, for each bee i, s_i falls in the set

$$\mathcal{S} = \{\text{U (``uninformed''); S (``streaker''); P (``passive leader'')}\}. \tag{2}$$

More specifically, scout individuals are set to have a streaker role when flying in the direction of the nest. Otherwise, they are defined as passive leaders. In this respect, we now introduce possible insect status transitions, which are summarized in panel (b) of Fig. 1. Of course, an uninformed bee can not become informed, so it can not change its status and will just follows the rest of the swarm. Status switches instead occur within the set of scout insects. In particular, let us first define for any point of the domain $\mathbf{x} \in \Omega$ the signed distance function $l_{\text{nest}}(\mathbf{x}) : \Omega \rightarrow \mathbb{R}_+ \cup \{0\}$, which is evaluated by solving the two-dimensional eikonal equation:

$$|\nabla l_{\text{nest}}(\mathbf{x})| = 1 \qquad \forall\, \mathbf{x} \in \Omega \tag{3}$$

with boundary conditions

$$\begin{cases} l_{\text{nest}}(\mathbf{x}) = 0, & \forall\, \mathbf{x} \in \partial\Omega_{\text{nest}}; \\[2mm] \dfrac{\partial l_{\text{nest}}(\mathbf{x})}{\partial \mathbf{n}} = 0, & \forall\, \mathbf{x} \in \partial\Omega \setminus \partial\Omega_{\text{nest}}, \end{cases} \tag{4}$$

where $\mathbf{n}$ is the unit vector locally normal to the domain boundary. It is useful to underline that, in other words, $l_{\text{nest}}(\mathbf{x})$ measures the length of the minimal path between any $\mathbf{x} \in \Omega$ and any point belonging to $\partial\Omega_{\text{nest}}$. Coherently with the previous experimental considerations, a streaker bee, say i, becomes a passive leader when it finds itself at the extreme frontal edge of the population, i.e., if, in mathematical terms,

$$l_{\text{nest}}(\mathbf{x}_i(t)) < \min_{\substack{k=1,...,N; k \neq i \\ \mathbf{x}_k(t) \in \Omega_i^{\text{vis}}(t)}} \{l_{\text{nest}}(\mathbf{x}_k(t))\},$$

being Ω_i^{vis} the visual region of individual i (see below). On the opposite, a passive leader, say again i, switches back to a streaker status if it finds itself at the trailing edge of the group of insects, i.e., if

$$l_{\mathrm{nest}}(\mathbf{x}_i(t)) > \max_{\substack{k=1,\ldots,N;k\neq i \\ \mathbf{x}_k(t)\in\Omega_i^{\mathrm{vis}}(t)}} \{l_{\mathrm{nest}}(\mathbf{x}_k(t))\}.$$

As most animal species, bees typically move and behave influenced by visual signals, captured by their large visual field, that covers almost the entire surrounding space. For the i-th insect (regardless of its status), we indeed denote by the unit vector $\mathbf{g}_i(t) \in S_1^2$ (being S_1^2 the unit 2-D ball) its actual gazing direction and by

$$\Omega_i^{\mathrm{vis}}(t) = \left\{ \mathbf{y} \in \Omega \,:\, |\mathbf{y} - \mathbf{x}_i(t)| \leq d_{\mathrm{vis}}, \frac{\mathbf{y} - \mathbf{x}_i(t)}{|\mathbf{y} - \mathbf{x}_i(t)|} \cdot \mathbf{g}_i(t) \geq \cos\theta_{\mathrm{vis}} \right\} \qquad (5)$$

its visual region, being d_{vis} and θ_{vis} the visual extension and the half visual angle, respectively (see Fig. 2). For sake of simplicity, we hereafter assume that the gaze of each bee is constantly aligned to its velocity, i.e.,

$$\mathbf{g}_i(t) = \frac{\mathbf{v}_i(t)}{|\mathbf{v}_i(t)|}, \qquad \text{for } i = 1,\ldots,N. \qquad (6)$$

However, individual gazing direction may also evolve slightly independently from the direction of flight: therefore, a proper evolution equation for $\mathbf{g}_i$ may be included as well, as done for instance in [17].

Bee dynamics. The collective movement of the swarm is described by a set of first-order ordinary differential equations (ODEs), which derives from a generic second-order model under the assumption of overdamped force-velocity response, which is a consistent hypothesis for living entities (e.g., cells, animals, humans, see the comments in [21, 30, 47]). In this respect, the i-th bee, with $i = 1, ..., N$, moves according to

$$\frac{d\mathbf{x}_i(t)}{dt} = \min\{v_{\mathrm{max}}, |\mathbf{v}_i(t)|\} \frac{\mathbf{v}_i(t)}{|\mathbf{v}_i(t)|}, \qquad (7)$$

where a control on its actual speed is done to avoid unrealistically high values, that may result also from plausible rules of movement. In this respect, v_{max} denotes the maximal admissible bee speed.

The insects then behave according to their role within the swarm. Coherently, we now define three different dynamics, each relative to an individual status. All of them are the sum of a given set of contributions, which can be in common for the entire population or characteristic of a single subgroup (and underlined in the following equations). In particular, for the generic i-th bee, we have

$$\begin{aligned}
\mathbf{v}_i(t) &= \mathbf{v}_i^{\mathrm{avoid}}(t) + \mathbf{v}_i^{\mathrm{group}}(t) + \mathbf{v}_i^{\mathrm{boundary}}(t) + \mathbf{v}_i^{\mathrm{rand}}(t) + \underline{\mathbf{v}_i^{\mathrm{align}}(t)}, \ \text{if } i : s_i(t) = \mathrm{U}; \\
\mathbf{v}_i(t) &= \mathbf{v}_i^{\mathrm{avoid}}(t) + \mathbf{v}_i^{\mathrm{group}}(t) + \mathbf{v}_i^{\mathrm{boundary}}(t) + \mathbf{v}_i^{\mathrm{rand}}(t) + \underline{\mathbf{v}_i^{\mathrm{streak}}(t)}, \ \text{if } i : s_i(t) = \mathrm{S}; \\
\mathbf{v}_i(t) &= \mathbf{v}_i^{\mathrm{avoid}}(t) + \mathbf{v}_i^{\mathrm{group}}(t) + \mathbf{v}_i^{\mathrm{boundary}}(t) + \mathbf{v}_i^{\mathrm{rand}}(t) + \underline{\mathbf{v}_i^{\mathrm{passive}}(t)}, \ \text{if } i : s_i(t) = \mathrm{P}.
\end{aligned}$$
$$(8)$$

We now comment each term in Eq. (8), starting from those active for all individuals.

The repulsive velocity component $\mathbf{v}^{\mathrm{avoid}}$ models the tendency of all bees of staying sufficiently far away from their neighbours, typically in order to avoid physical collisions and to maintain a minimal comfort space within the swarm. The term $\mathbf{v}^{\mathrm{group}}$ instead implements the desire of each individual to keep a connection with the groupmates, i.e., to remain close enough to the rest of the population. For the generic i-th insect, regardless of its status, both behaviors are described by proper kernels $\mathbf{H}_{ij}^{\mathrm{avoid}}, \mathbf{H}_{ij}^{\mathrm{group}} : \mathbb{R}^2 \times \mathbb{R}^2 \longmapsto \mathbb{R}^2$, which define its pairwise interaction instances with the generic j-th individual belonging to one of the following interaction sets:

$$
\begin{aligned}
\mathcal{N}_i^{\mathrm{avoid}}(t) &= \{j = 1, ..., N, j \neq i : \mathbf{x}_j(t) \in \Omega_i^{\mathrm{vis}}, 0 < |\mathbf{r}_{ij}(t)| \leq d_{\mathrm{avoid}}\}; \\
\mathcal{N}_i^{\mathrm{group}}(t) &= \{j = 1, ..., N, j \neq i : \mathbf{x}_j(t) \in \Omega_i^{\mathrm{vis}}, d_{\mathrm{avoid}} < |\mathbf{r}_{ij}(t)| \leq d_{\mathrm{group}}\},
\end{aligned}
\tag{9}
$$

where $\mathbf{r}_{ij}(t) := \mathbf{x}_j(t) - \mathbf{x}_i(t)$. In (9), d_{avoid} is a measure of the comfort space that each insect tries to preserve, whereas d_{group} is assumed to be equal to d_{vis}, i.e., the bees tend to keep a connection with the groupmates within their visual region, see Fig. 3 (a). Further, we assume that the above-introduced kernels do not depend on the specific couple of bees, i.e., $\mathbf{H}_{ij}^{\mathrm{avoid}} = \mathbf{H}^{\mathrm{avoid}}$ and $\mathbf{H}_{ij}^{\mathrm{group}} = \mathbf{H}^{\mathrm{group}}$ for any pair (i, j), that the resulting velocity contributions have an effect on the direction ideally connecting the interacting insects and finally that they depend on individual relative distance. In this respect, we can write:

$$
\mathbf{v}_i^{\mathrm{avoid}}(t) = \sum_{j \in \mathcal{N}_i^{\mathrm{avoid}}(t)} \mathbf{H}^{\mathrm{avoid}}(\mathbf{x}_j(t), \mathbf{x}_i(t)) = \sum_{j \in \mathcal{N}_i^{\mathrm{avoid}}(t)} h^{\mathrm{avoid}}(|\mathbf{r}_{ij}(t)|) \frac{\mathbf{r}_{ij}(t)}{|\mathbf{r}_{ij}(t)|}
$$

$$
\mathbf{v}_i^{\mathrm{group}}(t) = \sum_{j \in \mathcal{N}_i^{\mathrm{group}}(t)} \mathbf{H}^{\mathrm{group}}(\mathbf{x}_j(t), \mathbf{x}_i(t)) = \sum_{j \in \mathcal{N}_i^{\mathrm{group}}(t)} h^{\mathrm{group}}(|\mathbf{r}_{ij}(t)|) \frac{\mathbf{r}_{ij}(t)}{|\mathbf{r}_{ij}(t)|},
$$
$$
\tag{10}
$$

being again $\mathbf{r}_{ij}(t) := \mathbf{x}_j(t) - \mathbf{x}_i(t)$. To implement the desired phenomenology, the function h^{avoid} (respectively, h^{group}) has to be non positive (respectively, non negative) in its entire domain, i.e., $h^{\mathrm{avoid}} : \mathbb{R}_+ \longmapsto \mathbb{R}_- \cup \{0\}$ (respectively, $h^{\mathrm{group}} : \mathbb{R}_+ \longmapsto \mathbb{R}_+ \cup \{0\}$). In principle, there are many possible forms for such interaction laws. In particular, the avoidance bee behavior is hereafter described by a classical Newtonian-type short-range hyperbolic kernel

$$
h^{\mathrm{avoid}}(|\mathbf{r}_{ij}(t)|) = f_{\mathrm{avoid}} \left(\frac{1}{d_{\mathrm{avoid}}} - \frac{1}{|\mathbf{r}_{ij}(t)|} \right),
\tag{11}
$$

which has been employed in other particle models. For instance, it has been used by Diwold and coworkers to reproduce the collective flight of red dwarf honeybees (cf. [29], Eq. (1)) and by Chen and Kolokolnikov to study predator-swarm interactions (cf. [12], Eq. (1.1) and the references below). Repulsive kernels with similar trends (i.e., which go to infinity as $|\mathbf{r}_{ij}|^\alpha$, with $\alpha < 0$, when $|\mathbf{r}_{ij}| \to 0$, being $|\mathbf{r}_{ij}|$ the distance between two interacting agents) have been implemented also in the case of discrete approaches for zebrafish embryogenesis [25] and endothelial patterning on polymers [41]. In (11), the positive parameter $f_{\mathrm{avoid}} \in (0, +\infty)$, with units m^2/s, defines the slope of the hyperbolic function h^{avoid}.

On the other hand, long-range attraction between bees is assumed to have the

following parabolic form:

$$h^{\text{group}}(|\mathbf{r}_{ij}(t)|) = 4 f_{\text{group}} \frac{(d_{\text{group}} - |\mathbf{r}_{ij}(t)|)(|\mathbf{r}_{ij}(t)| - d_{\text{avoid}})}{(d_{\text{group}} - d_{\text{avoid}})^2}. \tag{12}$$

We do not use linear Hooke-like attraction laws, such as those introduced in some of the previously cited works dealing with swarming, e.g., [12, 29], since we hypothesize that the attractive stimulus is negligible when two bees are very close and, after a maximum, it decreases again to zero at d_{group}, which is taken to be the margin of the visual field. Finally, according to us, it is plausible that pairs of insects falling substantially apart one from each other do not have a significant mutual influence. The exact form of h^{group} is taken such that its maximum is given by the positive coefficient $f_{\text{group}} \in (0, +\infty)$, which has units m/s, and located in the middle of the interval $(d_{\text{avoid}}, d_{\text{group}})$. Analogous attraction functions has been used in the case of other particle models relative to bee and cell dynamics, see [3, 15–17] and references therein. It is also useful to underline that, according to the above-introduced kernels h^{avoid} and h^{group}, which are plotted in Fig. 3 (b), and to the corresponding interaction sets $\mathcal{N}^{\text{avoid}}$ and $\mathcal{N}^{\text{group}}$, two individuals do not interact (i) when they do not see each other and (ii) when they are exactly at the comfort distance d_{avoid}. It is finally useful to underline that the pair of coefficients f_{avoid} and f_{group} have a clear mathematical meaning, as commented above, but not a direct and measurable experimental counterpart. In this respect, their estimate has required a detailed parameter study, as discussed in the Appendix.

We then include a velocity term that implements the intention of bees to remain sufficiently distant from the domain boundary (which may represent, e.g., architectural structures or natural obstacles). In accordance to the case of pedestrians [17], such a migratory contribution enters the picture when the i-th individual (regardless of its status) is close enough, i.e., at a maximal distance hereafter defined with the coefficient d_{boundary}, to a boundary:

$$\mathbf{v}_i^{\text{boundary}}(t) = \begin{cases} a_{\text{boundary}} \exp\left(\dfrac{d_{\text{boundary}} - l_{\text{boundary}}(\mathbf{x}_i(t))}{b_{\text{boundary}}}\right) \mathbf{n}_{\text{boundary}}(\mathbf{x}_i(t)), \\[2ex] \quad \text{if } l_{\text{boundary}}(\mathbf{x}_i(t)) < d_{\text{boundary}}; \\[2ex] \mathbf{0}, \qquad\qquad \text{otherwise,} \end{cases} \tag{13}$$

where

$$\mathbf{n}_{\text{boundary}}(\mathbf{x}_i(t)) = \frac{\nabla l_{\text{boundary}}(\mathbf{x}_i(t))}{|\nabla l_{\text{boundary}}(\mathbf{x}_i(t))|} \tag{14}$$

is the unit vector directed from the nearest point of the domain boundary to the actual position of the insect i. $l_{\text{boundary}}(\mathbf{x}_i(t)) : \Omega \to \mathbb{R}_+ \cup \{0\}$ is in fact the distance function

resulting from the following eikonal equation and relative boundary conditions:

$$
\begin{cases}
|\nabla l_{\mathrm{boundary}}(\mathbf{x})| = 1 & \forall\, \mathbf{x} \in \Omega; \\[2mm]
l_{\mathrm{boundary}}(\mathbf{x}) = 0, & \forall\, \mathbf{x} \in \partial\Omega \setminus \partial\Omega_{\mathrm{nest}}; \\[2mm]
\dfrac{\partial l_{\mathrm{boundary}}(\mathbf{x})}{\partial \mathbf{n}} = 0, & \forall\, \mathbf{x} \in \partial\Omega_{\mathrm{nest}}.
\end{cases}
\tag{15}
$$

We here remark that, despite the term defined in (13), proper boundary conditions are needed. More specifically, we hereafter assume that when a bee touches a part of the domain not occupied by the nest, it stops, whereas it is taken out from the simulation when reaches a point of the target nest.

For each insect i, a fluctuation velocity term is added as well. It is given by a vector $\mathbf{v}_i^{\mathrm{rand}}$, whose modulus and direction are, at any time t, random variables which uniformly fall within the ranges of values $[0, v_{\mathrm{mean}}/10]$ and $[0, 360°)$, respectively (see below for the meaning of v_{mean}).

We now turn to describe the velocity components characteristic of the different bee subgroups. First, $\mathbf{v}_i^{\mathrm{align}}$ is an alignment term typical of the following individuals which, being uninformed of the position of the new nest, are only able to synchronize their flight with selected sets of mates. In this respect, for the i-th follower insect we define

$$
\mathbf{v}_i^{\mathrm{align}}(t) = v_{\mathrm{mean}} \frac{< \mathbf{v}_j(t) >_{j \in \mathcal{N}_i^{\mathrm{align}}(t)}}{|< \mathbf{v}_j(t) >_{j \in \mathcal{N}_i^{\mathrm{align}}(t)}|},
\tag{16}
$$

where v_{mean} denotes the characteristic speed of uninformed bees and

$$
< \mathbf{v}_j(t) >_{j \in \mathcal{N}_i^{\mathrm{align}}(t)} = \frac{1}{\#\mathcal{N}_i^{\mathrm{align}}(t)} \sum_{j \in \mathcal{N}_i^{\mathrm{align}}(t)} \mathbf{v}_j(t)
\tag{17}
$$

is the mean of the velocities of the groupmates falling within the alignment set $\mathcal{N}_i^{\mathrm{align}}(t)$, denoting by $\#$ its cardinality. In this respect, we propose four alternative definitions of $\mathcal{N}_i^{\mathrm{align}}$, in accordance with the different experimental hypotheses:

HP A1 - the i-th uninformed bee synchronizes its flight with the follower and the streaker individuals that are sufficiently fast and close to its position. This results in

$$
\begin{aligned}
\mathcal{N}_i^{\mathrm{align}}(t) \;=\; & \{j = 1, \ldots, N, j \neq i : s_j(t) \in \{\mathrm{U}, \mathrm{S}\}, \mathbf{x}_j(t) \in \Omega_i^{\mathrm{vis}}, \\
& 0 < |\mathbf{r}_{ij}(t)| \leq d_{\mathrm{align}}, |\mathbf{v}_j(t)| > |\mathbf{v}_i(t)|\},
\end{aligned}
\tag{18}
$$

where again $\mathbf{r}_{ij}(t) := (\mathbf{x}_j(t) - \mathbf{x}_i(t))$;

HP A2 - the i-th uninformed bee aligns to the faster groupmates, regardless of their status, provided that they are close enough, i.e.,

$$
\begin{aligned}
\mathcal{N}_i^{\mathrm{align}}(t) \;=\; & \{j = 1, \ldots, N, j \neq i : \mathbf{x}_j(t) \in \Omega_i^{\mathrm{vis}}, \\
& 0 < |\mathbf{r}_{ij}(t)| \leq d_{\mathrm{align}}, |\mathbf{v}_j(t)| > |\mathbf{v}_i(t)|\};
\end{aligned}
\tag{19}
$$

HP A3 - the i-th uninformed bee synchronizes its flight to all insects falling within a given

neighborhood, regardless of their status and speed. In mathematical terms:

$$
\begin{aligned}
\mathcal{N}_i^{\text{align}}(t) \quad = \quad & \{j = 1, \ldots, N, j \neq i : \mathbf{x}_j(t) \in \Omega_i^{\text{vis}}, \\
& 0 < |\mathbf{r}_{ij}(t)| \leq d_{\text{align}}\},
\end{aligned} \tag{20}
$$

HP A4 -   the i-th uninformed bee synchronizes its flight with the follower and the streaker individuals that fall within a given regions, regardless of their velocity:

$$
\begin{aligned}
\mathcal{N}_i^{\text{align}}(t) \quad = \quad & \{j = 1, \ldots, N, j \neq i : s_j(t) \in \{\text{U,S}\}, \mathbf{x}_j(t) \in \Omega_i^{\text{vis}}, \\
& 0 < |\mathbf{r}_{ij}(t)| \leq d_{\text{align}}\}.
\end{aligned} \tag{21}
$$

In all cases, d_{align} defines the extension of the alignment region. As discussed in the following, $d_{\text{align}} \in (d_{\text{avoid}}, d_{\text{group}})$, i.e., the flight synchronization set of an individual intersects those relative to its pairwise interactions with the groupmates. This assumption implies that each uninformed bee can simultaneously align to and avoid or be attracted by another individual, see Fig. 3 (a). Further, we remark that, in the case of hypotheses A1 and A4, the passive leaders are not taken into account by the follower bees, as assumed in the biological literature [46, 48]. However, it is useful to underline that the explanation of such a phenomenon is far to be understood. For instance, it is hypothesized that the passive leaders make themselves invisible to their groupmates by flying either close to the ground or backlight with respect to the sun or hidden in the middle the rest of the cloud (see again [46, 48]). In this respect, given the absence of detailed experimental evidence and in order to avoid further model overcomplications, we here opt to focus only on the typology of the flight of the informed insects (i.e., "back-and-forth" vs. "go-and-stop") and not on the zones of the swarm where such characteristic movements are performed. This issue would require further empirical investigations and, from a mathematical point of view, the introduction of three-dimensional settings. However, planar domains to describe bee swarming, including the dynamics of the leader individuals, are consistently employed across the theoretical literature (refer, for instance, to [11, 29]).

In Eq. $(8)_2$, $\mathbf{v}_i^{\text{streak}}$ describes the characteristic motion of the scout bees with a streaker status, i.e., when they fly at high speed in the direction of the nest thereby behaving as guidance leaders for the rest of the swarm. In particular, for the i-th streaker insect (i.e., $i : s_i(t) = \text{S}$), we set:

$$
\mathbf{v}_i^{\text{streak}}(t) = -v_{\max} \frac{\nabla l_{\text{nest}}(\mathbf{x}_i(t))}{|\nabla l_{\text{nest}}(\mathbf{x}_i(t))|}, \tag{22}
$$

where ∇l_{nest} and $v_{\max}$ have been introduced in (3) and (7), respectively. Equation (22) implies that each streaker individual performs a flight that, at each time instant t, is aligned to the direction minimizing the distance between its position and the target nest, i.e., it moves along the *optimal trajectory*. In this respect, we here remark that the use of eikonal equations is usually employed in methods related to the computation of optimal paths. More specifically, Eq. (22) has the advantage that it can be used regardless the complexity of the domain, with straightforward extension to the case of non-planar geometries. Further comments on this aspect can be found in [17], where different approaches for evaluating individual minimal trajectories to a given target are discussed as well.

We then propose two alternative hypothesis for the characteristic behavior of scout bees when they take a passive leader role:

HP L1 - on one hand, they are assumed to slowly fly back towards the rear edge of the swarm, in order to slightly affect the movement of the rest of the groupmates. In this respect, for the i-th passive leader bee, we set

$$\mathbf{v}_i^{\text{passive}}(t) = v_{\text{mean}} \frac{\dfrac{\mathbf{x}_{\bar{k}}(t) - \mathbf{x}_i(t)}{|\mathbf{x}_{\bar{k}}(t) - \mathbf{x}_i(t)|} + \dfrac{\nabla l_{\text{nest}}(\mathbf{x}_i(t))}{|\nabla l_{\text{nest}}(\mathbf{x}_i(t))|}}{\left| \dfrac{\mathbf{x}_{\bar{k}}(t) - \mathbf{x}_i(t)}{|\mathbf{x}_{\bar{k}}(t) - \mathbf{x}_i(t)|} + \dfrac{\nabla l_{\text{nest}}(\mathbf{x}_i(t))}{|\nabla l_{\text{nest}}(\mathbf{x}_i(t))|} \right|}, \tag{23}$$

where $\bar{k}$ is such that

$$l_{\text{nest}}(\mathbf{x}_{\bar{k}}(t)) = \max_{\substack{k\,:\,s_k(t)=\text{U} \\ \mathbf{x}_k(t) \in \Omega_i^{\text{vis}}(t)}} l_{\text{nest}}(\mathbf{x}_k(t)),$$

i.e., $\bar{k}$ is the uninformed insect farthest from the target nest;

HP L2 - on the other hand, we hypothesize that the passive leaders stop and wait for the passage of the rest of the population. For the i-th passive leader, we indeed set

$$\mathbf{v}_i^{\text{passive}}(t) = \mathbf{0}. \tag{24}$$

The entire model parameter setting used in the following simulations is summarized in Table 1, while in the Appendix we will detail how they have been estimated.

3. Numerical results

The numerical results proposed in this section will be divided in two parts. In the first Section 3.1, we will test different combinations of the alternative assumptions relative to the alignment mechanism of the uninformed bees and to the behavior of the passive leaders. By considering swarm dynamics within a simple rectangular domain, we will look at the rules of motion that result in a realistic migration of the insect cloud, which has to fly compactly and productively towards the nest. The effect of variations in the percentage of informed bees will be analyzed as well. Section 3.2 will be instead devoted to reproduce the collective phenomenology of the bee population in more complex environments, which involve domains with different obstacles.

3.1. Swarming in a large open-space domain

In this first set of simulations, we use a rectangular $[0, 200] \times [0, 200]$ m^2 domain Ω, where the target destination is constituted by the boundary segment $y \in [95, 105]$ on the right side of the domain, see Fig. 4. The measure of $\partial\Omega_{\text{nest}}$ is larger than the dimension of a real nest, since we here intend to describe the behavior of the swarm while approaching the new home and not the subsequent entrance mechanisms, that are driven by other processes (e.g., pheromone cues). The insect population is formed by $N = 500$ individuals (we recall that we are dealing with a planar section of a larger three-dimensional swarm). In particular, 480 of them are uninformed followers, while the remaining ones are scouts with an initial streaker role, i.e., $s_i(0) = \text{S}$ for $i \in \{481, ..., 500\}$. We here recall that uninformed bees are not allowed to change state, whereas the informed insects can switch between the streaker and the passive

leader status. The swarm is initially arranged in an almost round area centered at (100 m, 100 m) of radius equal to $r_0 = 4$ m, where the positions of the insects are randomly assigned, refer again to Fig. 4. In this respect, we account for a reasonable density of ≈ 8 bees/m^2 [48]; also the percentage of informed individuals, i.e., 4 % of the entire population, is in agreement with the experimental literature [49–51]. The initial gazing direction $\mathbf{g}_i(0)$ of each generic i-th bee is randomly generated as well.

The objective of the swarm is to reach the target destination. In this respect, the numerical realizations are stopped as soon as the last insect touches a point of $\partial\Omega_{\mathrm{nest}}$, i.e., at a time denoted with t_{F}. The dynamics of the bee population resulting from different combinations of the individual behavioral hypotheses outlined in Section 2 are classified according to the following criteria:

Definition 3.1. The swarm undergoes a *directionally productive motion* towards the nest if

$$E_{\mathrm{swarm}} = \lim_{t\to\infty} l_{\mathrm{nest}}(\mathbf{x}_{\mathrm{swarm}}(t)) = 0, \tag{25}$$

where $\mathbf{x}_{\mathrm{swarm}}(t) = \dfrac{\sum_{i=1}^{N} \mathbf{x}_i(t)}{N}$ is the center of mass of the bee cloud and l_{nest} is the distance function introduced in Eq. (3).
The swarm undergoes a *coherent and collective flight* if

$$C_{\mathrm{swarm}} = \max_{t>0} \frac{a_{\mathrm{swarm}}(t)}{a_{\mathrm{R}}} < 2, \tag{26}$$

where $a_{\mathrm{swarm}}(t)$ is a measure of the space extension[1] of the bee cloud at time t and a_{R} is equal to $\pi(r_0)^2$, i.e., the area of the round region initially containing all individuals. The swarm undergoes a *collective and productive flight* towards the nest if both conditions (25) – (26) are satisfied.

The quantity defined in Eq. (26) is able to give an indication of the presence of dispersed insects, i.e., of bees unable to correctly synchronize their movement with the rest of the group. In fact, our simulation results have consistently shown that if, at a given time t, the surface of the insect cloud is twice the reference initial area a_{R} (or even more), then there is at least a follower bee that actually has no groupmate within its alignment set which means that it has lost.

Figs. 5 – 7 summarize the results obtained by the different combinations of the individual behavioral hypotheses. In particular, for each pair of assumptions, we have run 10 independent numerical realizations, given the presence of randomness both in the initial position of the bees and in their dynamics due to the velocity term $\mathbf{v}^{\mathrm{rand}}$. We can observe that in all cases the distance $l_{\mathrm{nest}}(\mathbf{x}_{\mathrm{swarm}}(t))$ between the swarm center of mass and the nest decreases almost linearly (see also the inset graph in Fig. 5 (a)). In particular, it becomes null in a finite time (< 14 seconds), as E_{swarm} is zero. However, as shown in the plot of C_{swarm} in Fig. 5 (b), only under hypotheses (A3, L1), (A3, L2) and (A4, L2), the flight of the insect population is completely synchronized and therefore collective in all realizations. In the other cases, as also shown in the representative snapshots in Figs. 6 and 7, at least one uninformed bee does not correctly align to

---

[1]The spatial extension of the swarm is evaluated by the Matlab (the MathWorks®) function `boundary`. More specifically, this function returns the area enclosed by the single conforming 2-D boundary containing of a given set of discrete particles. For further details, we refer to Matlab manuals and tutorials.

the rest of the swarm, flying away from the groupmates. In these situations, the scout bees have to take time to reach/wait for the dispersed individual(s) and to guide it (them) towards the nest: the experimentally-observed compactness of the insect cloud is therefore not maintained. From the graph in Fig. 5 (b), it can be further noticed that bee dispersion is more significant in the case of assumptions (A2, L1) and (A2, L2), i.e., when the uninformed bees align to the faster groupmates, regardless of their status.

Taking all the results together, we can state that in our model alignment mechanisms involving a control over groupmate velocity do not certainly imply directionally productive and collective swarm dynamics. An efficient and coordinate flight is instead reproduced if the follower individuals synchronize their movement (i) to all insects sufficiently close to their position, regardless of their status and of the behavior of the passive leaders, or (ii) only to close enough uninformed and streaker groupmates, provided the fact that the passive leaders stop upon reaching the front of the cloud. In particular, it is somehow worth to remark that, in the case of hypotheses A1 and A4, passive leader bees are not considered for the alignment mechanism: however, they determine the flight of the follower groupmates by affecting the other velocity components (e.g., collision avoidance and attraction).

We now turn to describe and compare in more details selected characteristics of swarm dynamics under the plausible combinations of behavioral assumptions. In this respect, Fig. 8 shows the time-evolution of the amount of bees belonging to each subpopulation in the different cases. As it is possible to observe, the number of follower individuals remains obviously constant whereas, transitions between streaker and passive leader states continuously occur. In particular, under the coupled hypotheses (A3, L1), the amount of streaker insects remains substantially higher that the number of passive leaders during the entire migration (the former falling within the range 14-20, the latter within the range 0-6). On the opposite, in the case of assumptions (A3, L2) and (A4, L2) (i.e., when the passive leaders are assumed to stop and wait for the rest of the colony), the fluctuations in the cardinality of two subgroups of scout bees are more significant: for instance, the amount of streakers can drop and be almost equal to the number of passive leaders.

Fig. 9 finally compares the trajectories of representative scout bees under the different assumptions resulting in realistic swarm dynamics. In particular, under the coupled hypotheses (A3, L1), it is straightforward to notice the short-time backward movement of the informed individual during its passive leader status. It is also interesting to observe that under the assumptions (A3, L2) and (A4, L2), the scout bees, when passive leaders, do not completely stop but rather still move as a consequence of the velocity components which are still active (i.e., those relative to attractive/repulsive interactions and to random fluctuations).

Variations in the percentage of scout bees. As seen, the collective migration of bee swarms is guided by few informed individuals, that are able to diffuse information of the nest location within the rest of the population. An interesting question is indeed relative to the consistency of the flight directional efficiency upon variations in the ratio between the number of individuals having the different roles within the colony.

In this respect, we now study the dynamics of insect clouds characterized by different numbers of scouts and of overall components. In particular, we employ the same domain of the previous section and the rules of motion defined in Section 2: however, only the combinations of assumptions that have resulted in a plausible system phenomenology are hereafter used, i.e., the pairs (A3, L1), (A3, L2), and (A4, L2). As

initial data, the bees are again randomly disposed in round regions, whose radius is chosen, in each case, to maintain the density of 8 bees/m^2. All scout individuals have a streaker status whereas the initial bee gazing direction is randomly assigned.

As it is possible to observe in Fig. 10, for a given group size, i.e., for a fixed N, the directionally productive component of swarm movement increases (i.e., E_{swarm} decreases) as the percentage of informed individuals increases. Furthermore, still from the same plot, we can notice that the higher the overall number of bees is, the smaller the proportion of informed individuals necessary is in order to have an efficient migration towards the nest. In particular, substantially large swarms require a very small set of scout bees to reach the target destination.

These results are observed for all the tested combinations of behavioral assumptions (even if for clarity we represented only the case relative to the pair (A4, L2), being completely robust also in the case of independent simulations in the different settings (in each case, the standard deviation deriving from 10 simulations is < 1% and therefore not represented in the graphs). We also remark that in the cases of full productive swarming (i.e., when $E_{swarm} \approx 0$) no bee dispersion occurs (i.e., $C_{swarm} < 2$), in agreement with the outcomes presented in the previous subsection.

As it will be commented in more details in the conclusive part of the paper, analogous quite surprising results have been obtained in the works by Couzin et al. [19] and by Fetecau and Guo [31], where similar microscopic/discrete models have been employed to describe collective swarming.

3.2. Swarming in more realistic situations

Finally, we turn to asses the applicability of our model in real-world situations by means of representative numerical results involving more complex environments.

In particular, referring to Figs. 11 and 12, we deal with domains characterized either by a structural obstacle or by a bottleneck, placed in between the initial position of the swarm and the target destination. Such environmental elements may represent architectural buildings or trees that the insect cloud has to avoid during its migration. Hereafter, the bee population is still assumed to be composed of $N = 500$ individuals, which are initially subdivided into 480 uninformed insects and 20 streakers. As usual, the initial configuration of the swarm consists of a circle of radius $r_0 = 4$ m with bee position and gazing direction randomly assigned. Again we test the coupled hypothesis (A3, L1), (A3, L2), and (A4, L2). The center of the nest is located at the same y-coordinate of the initial center of mass of the insect cloud.

As it is possible to observe in Figs. 11 and 12, in both situations, the swarm has to slightly deflect its direction of movement and to deform to pass the structural elements and reach the target destination. In particular, in the case of the square obstacle, the bees located at the bottom part of the population are pressed towards the center of the swarm by the repulsive velocity $\mathbf{v}^{boundary}$. We indeed have an increasing density of insects in the center of the cloud. However, the productive direction of flight is still maintained. Once passed the structural element, the compressed area of the swarm slightly relaxes and an almost homogeneous density of bees is recovered.

Referring to Fig. 12, when approaching the bottleneck, the swarm is instead substantially stretched horizontally and compressed vertically, i.e., it switches from a round shape to a ellipsoidal geometry, with shorter axis along the y-direction of the domain. Interestingly, after passing the bottleneck, there is only a slight relaxation of the insect cloud, which does not acquire again a fully-round configuration. The underlying

13

rationale is that, even when the colony has an elongated shape, the component bees are at a sufficient (but not excessive) distance one from another and therefore there is no reason to spend energy to further reorganize.

In both domains configurations, the swarm finally redirect again its coordinate flight to reach the target destination.

The above-described phenomenologies are observed under the three tested coupled hypotheses, with slight differences in the morphological transitions of the swarm. However, we remark that, in all settings, there is no bee dispersion.

The results presented in this section allow us to conclude that the behavioral rules of bees (A3, L1), (A3, L2), and (A4, L2) give a realistic swarming not only in open-space simple domains but also in more complex scenarios. In particular, our model, under such plausible hypotheses, is able to capture autonomous morphological reorganizations and changes of flight direction of the insect cloud, necessary to preserve its compactness and to reach the target destination.

4. Discussion

The collective motion of groups of animals has recently attracted an increasing interest in the modeling community. Particularly intriguing is the swarming of bee populations towards a new nest. In fact, such a characteristic migration is led by few informed/scout individuals, which have previously explored the possible new home and therefore are able to guide the groupmates towards the target destination. However, also from an experimental point of view, little is known on the behavioral rules underlying the coordinated flight of bee swarms. In particular, it is not completely clear how the information on the nest location spreads within the population and what are the exact dynamics of the informed individuals.

The aim of this work has been indeed to test alternative assumptions and to find out those resulting in realistic swarming phenomenologies. To do this, we employed a discrete mathematical model, where each insect has been individually represented by a material point and assigned a given behavioral status (i.e., streaker, passive leader or uninformed). The subgroups of bees have in common some general rules of motility, such as the tendency to remain within the population while keeping a comfort distance from the other components. Other principles of motion are instead characteristic of a single subpopulation, such as the ability if uninformed bees to synchronize their flight with the surrounding groupmates. These ideas have been translated in a mathematical model based on a set of first-order ODEs, each of them describing the evolution of the position of an insect.

The resulting model has been used to test combinations of alternative assumptions underlying the synchronization mechanisms of uninformed bees and the individual behavior of passive leader bees. In particular, our results have shown that a productive collective flight of the swarm is only possible if the uniformed individuals synchronize their movement (i) to all insects sufficiently close to their position regardless of their status and velocity and of the dynamics of the passive leaders (i.e., coupled assumptions (A3, L1) and (A3, L2)) or (ii) only to close enough follower and streaker groupmates, provided the fact that the passive leaders stop upon reaching the front of the swarm (i.e., coupled assumptions (A4, L2)). Other sets of hypotheses have produced the unrealistic phenomenon of bee dispersion, i.e., at least one follower individual is not able to synchronize its movement with the rest of the swarm during the entire flight, thereby flying away and affecting the migration of the informed bees and

14

eventually of the entire population.

Once the most plausible behavioral assumptions have been identified, we have turned to analyze the effect of variations in the number of scout bees. Interestingly, we have found that larger swarms require fewer scout individuals to compactly reach the target destination. This quite surprising outcome is in agreement with the results obtained by similar models [19, 31]. However, it is useful to remark that from experimental observations it is known that, regardless the size of the population, the fraction of informed insect typically falls in the range 3%-5%. In this respect, we can speculate that, although in principle the percentage of scout bees could decrease, their amount may be established also by other social dynamics of the swarm not involving migration issues. For instance, a sufficiently high number of scout bees could be necessary to explore the environment to find a new home in a substantially short time.

With the last set of simulations, we have finally provided the fact that our model, with the selected combinations of bee behavioral assumptions, is able to capture swarm dynamics in more complex scenarios, that may require morphological rearrangements of the insect cloud to pass structural elements and significant changes of flight directions.

4.1. Comparison with pertinent literature

The description of the collective and coordinated dynamics of groups of animals is a challenging topic for theoretical researchers. Populations of intelligent living entities are in fact *complex systems*, since the component individuals are not passively dragged by external forces but rather they undergo active decision-based dynamics, so that the use of classical passive mechanics is no longer sufficient. The overall evolution of the group then emerges from the rules governing the individual behavior. In this respect, the mathematical and computational literature in this field presents indeed a wide range of approaches.

For instance, *microscopic* models (also called individual-based models, IBMs) describe a group of animals as a collection of isolated agents: each of them is individually considered, assimilated for instance to a point particle or a quasi-rigid disk and followed during motion. More specifically, a first subgroup of microscopic models is represented by the so-called *cellular automata* (CA), where each animal is set to behave according to phenomenological algorithmic rules, that depend on its individuality and/or on the surrounding environment. Another subtype of microscopic approach involves instead *discrete* models: they rely on classical Newtonian laws of point mechanics, as the motion of each agent is defined by a first- or a second-order ordinary differential equation (ODE).

However, when the number of component individuals is significantly large, as in the case of fishes [42] or myxobacteria [33, 37], microscopic methods become computationally expensive and therefore different approaches are needed. In this respect, *continuous models*, characteristic of a *macroscopic* point of view, rely on the definition of a proper density of agents, which evolves following (typically nonlinear) partial differential equations (PDEs), which implement conservation laws and require phenomenological assumptions for their closure, see for example [5, 55–57].

A bridge between the microscopic word and the macroscopic representation of animal systems is represented by *kinetic* models. Characteristics of a *mesoscopic* point of view, they are able to derive, employing hydrodynamic arguments, Boltzmann-like evolution laws for statistical distribution functions, which describe position and veloc-

ity of the components of the population of interest [7, 9, 38].

The model presented in this article belongs to the class of microscopic/discrete methods. Since some of them are devoted to reproduce selected features of bee swarming, it is important to discuss differences and similarities with respect to our approach, mainly in the term relative to the behavior of scout/informed individuals. Entering in more details, in [31], Fetecau and Guo implement a second-order model with differentiation between informed and uninformed bees. More specifically, the formers do not interact with their groupmates and move faster towards the target destination according to two alternative hypothesis: (i) they streak with a constant acceleration or (ii) they fly with a constant speed. In both cases, when such informed individuals reach the leading edge of the cloud, they come back to the rear of the population being 10 time less visible. Each uninformed insect instead undergoes attractive and repulsive stimuli, described by a Morse potential, and alignment mechanisms, which involve its two-fold faster neighbors. Bee dynamics account for a random component as well, which is active only when the interaction of an individual with the rest of the swam is low enough. The authors also introduce a visual field for each bee, given by a planar cone which is constantly aligned to the direction of motion and formed by two regions: a central cone where the other individuals are set to be seen directly, and therefore assigned a unit weight, and a peripheral area where the other individuals are set to be seen partially, and therefore assigned a lower weight. In our model, a peripheral vision is not considered, since it is known from biology that the compound eyes of bees cover most of the front and of the sides of their head, assuring an almost homogeneous vision. The model by Fetecau and Guo is therefore based on behavioral rules similar to the pairs (A1, L1) and (A2, L1) employed in our article. Interestingly, in both works, such hypotheses result in a directionally efficient swarming: however, we have discarded the two combinations of assumptions as a consequence of the lack of a consistent compactness of the insect cloud.

As in the case of the work by Fetecau and Guo, also in [40], a set of informed bees is defined within the swarm and assigned a back-and-forward motion within the swarm, in order to diffuse the information of the productive direction to the overall population. Such a first-order model also involves attraction, repulsion, and alignment. In particular, the cohesion velocity contribution is modeled as a vector pointing from the position of each bee to the center of mass of the set of neighboring insects which fall within its visual distance. In this respect, we here preferred to implement pairwise interaction kernels, since it is difficult to establish whether a bee exactly knows the position of the center of mass of the rest of groupmates. The alignment rule instead relies on an Euclidean metric-based assumption, namely each bee is set to synchronize its movement with all the seen groupmates (regardless of their speed).

In [29], the authors describe both the decision-making process used by the house-hunting honeybees to find a new nest site and their guidance role within the rest of the swarm. Focusing on the latter, we can notice that Diwold and colleagues employ a cohesion term that makes each bee attracted by the center of mass of the population only in the case of the presence of at least a fast enough individual within a given neighborhood. These authors also implement a topological metric-based alignment mechanism, i.e., a flight synchronization with a given number of closest fast individuals. The resulting model is then applied to compare the swarming of two different species of honeybees, namely *Apis Mellifera* and *Apis Florea*. In particular, while *A. Mellifera* is a cavity-nesting species, whereas *A. Florea* is an open-nesting species. This means that the *Apis Mellifera* has to find a roomy and comfortable homesite, protected from cold winds and from predators. Conversely, *A. Florea* usually nests on a shaded branch,

having less constraints in finding a suitable location.

A more general (i.e., not strictly related to bee dynamics) model is proposed in [19]. The authors here focus on two aspects: how information is transferred among moving groups of animals and how they can find an agreement when scout individuals suggest different moving directions to rest of the population. Such an approach still relies on the classical social principle of attraction/repulsion and alignment. As previously commented, one of their main results is related to the relationships between the percentage of informed bees and the flight efficacy of the swarm at different population sizes. The same research group also proposes a model that focuses on the pattern characteristic of animal populations [20]. Their approach includes a Morse potential and two additional terms: they are relative to self-propulsion and friction and their balance results in the capability of the system to reach an asymptotic collective speed (as it happens also in our model in given regimes of the free parameters).

Finally, the Cucker-Smale model (even with the inclusion of temporary leader emergence) accounts only for a term relative to a movement synchronization mechanism, which is affected by a communication rate that depends on the interindividual mutual distances [22, 23]. The model is of course able to capture flocking phenomenology.

Chen and Kolokolnikov instead presented in [12] a particle model able to capture selected features of predator-prey interactions in the case of a generic swarm. In their approach, each prey is attracted by its groupmates, whereas repulsive stimuli describe its intention to maintain a comfort space within the insect cloud and to fly away from the predator. The predator, in turn, is attracted by the preys. In more details, hyperbolic laws are implemented to describe repulsive dynamics (as in our model) while a linear short-range attraction is used for the individual cohesive behavior. The approach by Chen and Kolokolnikov is finally able to predict the shape of the swarm as well as the behavior of the predator in different regions of the model parameter space.

By reviewing the different works commented in this dissertation, we can conclude that the main features of a swarming phenomenology can be captured by minimal, i.e., two- or three-component, models. In fact, reasonable configurations of swarms (where the agents stabilize at given and finite mutual distances) can be obtained only by taking into account repulsive/attractive pairwise dynamics. The insertion of an aligned mechanism, such as the one we proposed in [3], is instead needed to get effective directional flights. Such simple models have also the advantage of being suitable for interesting analytical analysis and insight, e.g., on the properties of the steady states of the system as done by different groups [9, 10, 32].

In this respect, the inclusion of more sophisticated model ingredients, i.e., bee status differentiations and relative transitions and flight rules, is therefore not essential to reproduce basic collective dynamics of insect swarms. However, such model components have been here introduced in order to be as close as possible to experimental evidences and to find out reasonable assumptions at the basis of the still unknown bee behavior.

4.2. Further developments

The proposed model has investigated and tested different social mechanisms underlying the behavior of a bee swarm. However, our approach can be further improved in several directions. First, it would be useful to have a better comparison with experimental data. In particular, this would improve the quality of the work from two points of view: it could be possible to derive a more precise parameter estimate and we could

have a quantitative validation of the proposed theoretical results.

Further, a three-dimensional extension of the model would be a natural development. In fact, it would allow to better describe the dynamics of the informed bees which, when passive leaders, are also supposed to hide themselves along the top or the bottom region of the swarm in order to not significantly affect the flight of the groupmates, as hypothesized in the empirical literature [46, 48] and previously commented in this work.

References

[1] J. M. Graham (ed.), *The hive and the honey bee*, Dadant & Sons, Hamilton, IL, 1992.

[2] M. Beekman, R. L. Fathke, and T. D. Seeley, *How does an informed minority of scouts guide a honeybee swarm as it flies to its new home?*, Animal Behaviour 71 (2006), pp. 161–171.

[3] S. Bernardi, A. Colombi, and M. Scianna, *A discrete particle model reproducing collective dynamics of a bee swarm*, Comp. Biol. Med. 93 (2018), pp. 158–174.

[4] N. Boeddeker, L. Dittmar, W. Stürzl, and M. Egelhaaf, *The fine structure of honeybee head and body yaw movements in a homing task*, Proceedings of the Royal Society of London B: Biological Sciences 277 (2010), pp. 1899–1906.

[5] M. Burger, V. Capasso, and D. Morale, *On an aggregation model with long and short range interactions*, Nonlinear Analysis: Real World Applications 8 (2007), pp. 939–958.

[6] J. A. Cañizo, J. A. Carrillo, and F. Patacchini, *Existence of compactly supported global minimisers for the interaction energy*, Arch. Rational Mech. Anal. 217 (2015), pp. 1197–1217.

[7] J. A. Cañizo, J. A. Carrillo, and J. Rosado, *A well-posedness theory in measures for some kinetic models of collective motion*, Math. Models Methods Appl. Sci. 21 (2011), pp. 515–539.

[8] J. A. Carrillo, A. Colombi, and M. Scianna, *Adhesion and volume constraints via nonlocal interactions, lead to cell sorting*, J. Theor. Biol. 445 (2018), pp. 75–91.

[9] J. A. Carrillo, M. R. D'Orsogna, and V. Panferov, *Double milling in self-propelled swarms from kinetic theory*, Kinetic and Related Models 2 (2009), pp. 363–378.

[10] J. A. Carrillo, M. Fornasier, J. Rosado, and G. Toscani, *Asymptotic Flocking Dynamics for the kinetic Cucker-Smale model*, SIAM J. Math. Anal. 42 (2009), pp. 218–236.

[11] J. A. Carrillo, M. Fornasier, G. Toscani, F. Vecil, *Particle, kinetic, and hydrodynamic models of swarming*, in *Mathematical modeling of collective behavior in socio-economic and life sciences*, Birkhäuser, Boston, 2010, pp. 297–336.

[12] Y. Chen, and Theodore Kolokolnikov, *A minimal model of predator-swarm dynamics*, Journal of the Royal Society Interface 11 (2014), pp. 20131208.

[13] Y. Choi, R. Lui, and Y. Yamada, *Existence of global solutions for the Shigesada-Kawasaki-Teramoto model with weak cross-diffusion*, Discrete and Continuous Dynamical Systems 9(2003), pp. 1193–1200.

[14] Y. L. Chuang, M. R. D'Orsogna, D. Marthaler, A. L. Bertozzi, and L. Chayes, *State transitions and the continuum limit for a 2D interacting, self-propelled particle system*, Physica D 232 (2007), pp. 33–47.

[15] A. Colombi, M. Scianna, and L. Preziosi. *Coherent modelling switch between pointwise and distributed representations of cell aggregates*, J. Math. Biol. 74 (2017), pp. 783–808.

[16] A. Colombi, M. Scianna, and A. Tosin. *Differentiated cell behavior: a multiscale approach using measure theory*, J. Math. Biol. 71 (2015), pp. 1049–1079.

[17] A. Colombi, M. Scianna, and A. Alaia, *A discrete mathematical model for the dynamics of a crowd of gazing pedestrians with and without an evolving environmental awareness*, Comp. Appl. Math. 36 (2017), pp. 1113–1141.

[18] E. Conway and J. Smoller, *Diffusion and the predator-prey interaction*, SIAM Journal on Applied Mathematics 33 (1977), pp. 673–686.

[19] I. D. Couzin, J. Krause, N. R. Franks, and S. A. Levin, *Effective leadership and decision-making in animal groups on the move*, Nature, 433 (2005), pp. 513–516.

[20] I. D. Couzin, J. Krause, R. James, G. Ruxton, and N. Franks, *Collective memory and spatial sorting in animal groups*, J. Theor. Biol. 218 (2002), pp. 1–11.

[21] E. Cristiani, B. Piccoli, and A. Tosin, *Multiscale Modeling of Pedestrian Dynamics*, in *MS and A: Modeling, Simulation and Applications*, Vol. 12, Springer International Publishing, Berlin, 2014.

[22] F. Cucker and S. Smale, *On the mathematics of emergence*, Jpn. J. Math. 2 (2007), pp. 197–227.

[23] F. Cucker and S. Smale, *Emergent behavior in flocks,* IEEE Trans. Automat. Control, 52 (2007), pp. 852–862.

[24] M. R. D'Orsogna, Y. L. Chuang, A. L. Bertozzi, and L. S. Chayes, *Self-propelled particles with soft-core interactions: patterns, stability, and collapse*, Phys Rev Lett. 96 (2006), pp. 104302.

[25] E. Di Costanzo, R. Natalini, and L. Preziosi, *A hybrid matheatical model for self-organizing cell migration in the zebrafish lateral line*, J. Math. Biol., 71 (2015), pp. 171–214.

[26] P. Degond, S. Génieys, and A. Jüngel, *A steady-state system in non-equilibrium thermo-dynamics including thermal and electrical effects*, Mathematical methods in the applied sciences 21 (1998), pp. 1399–1413.

[27] P. Degond and S. Motsch, *Continuum limit of self-driven particles with orientation interaction*, Math. Models Methods Appl. Sci. 18 (2008), pp. 1193–1215.

[28] P. Degond and S. Motsch, *Large-scale dynamics of the Persistent Turing Walker model of fish behavior*, J. Stat. Phys. 131 (2008), pp. 989–1021.

[29] K. Diwold, T. M. Schaerf, M. R. Myerscough, M. Middendorf, and M. Beekman, *Deciding on the wing: in-flight decision making and search space sampling in the red dwarf honeybee Apis florea*, Swarm Intelligence 5(2011), pp. 121–141.

[30] D. Drasdo, *On selected individual-based approaches to the dynamics of multicellular systems*, in *Multiscale Modeling*, W. Alt and M. Griebel, eds., Birkhäuser, Basel, 2005, pp. 169–203.

[31] R. C. Fetecau and A. Guo, *A mathematical model for flight guidance in honeybees swarms*, Bull. Math. Biol. 74 (2012), pp. 2600–2621.

[32] R. C. Fetecau, Y. Huang, and T. Kolokolnikov, *Swarm dynamics and equilibria for a nonlocal aggregation model*, Nonlinearity, 24 (2011), pp. 2681–2716.

19

[33] H. Von Foerster, *Some remarks on changing populations*, in *The kinetics of cellular proliferation*, Grune and Stratton, New York, 1959, pp. 382–407.

[34] M. Fornasier, J. Haskovec, and G. Toscani, *Fluid dynamic description of flocking via Povzner-Boltzmann equation*, Physica D: Nonlinear Phenomena 240 (2011), 21–31, 2011.

[35] G. Galiano, A. Jüngel, and J. Velasco, *A parabolic cross-diffusion system for granular materials*, SIAM Journal on Mathematical Analysis 35 (2003), pp. 561–578.

[36] I. Giardina, *Collective behavior in animal groups: theoretical models and empirical studies*, HFSP Journal, 2 (2008), pp. 205–219.

[37] W. Gurney, S. Blythe, and R. Nisbet, *Nicholson's blowflies revisited*, Nature 287 (1980), pp. 17–21

[38] S. Y. Ha and J. G. Liu, *A simple proof of the Cucker-Smale flocking dynamics and mean-field limit*, Comm. Math. Sci. 7 (2009), pp. 297–325.

[39] S. Y. Ha and E. Tadmor, *From particle to kinetic and hydrodynamic descriptions of flocking,* Kinetic and Related Models 1 (2008), pp. 415–435.

[40] S. Janson, M. Middendorf, and M. Beekman, *Honeybee swarms: how do scouts guide a swarm of uninformed bees?*, Animal Behaviour 70 (2005), pp. 349–358.

[41] J. Joie, Y. Lei, T. Colin, M. C. Durrieu, C. Poignard, and O. Saut O (2013)*Modelling of migration and orientation of endothelial cells on micropatterned polymers*, research report INRIA RR-8252, 20 pp (2013). http://hal.inria.fr/docs/00/99/07/77/PDF/RR-discret2.pdf

[42] J. Kim, *Smooth solutions to a quasi-linear system of diffusion equations for a certain population model*, Nonlinear Analysis: Theory, Methods & Applications 8 (1984), pp 1121–1144.

[43] Y. Kuang and S. Gourley, *Wavefronts and global stability in a time-delayed population model with stage structure*, Proceedings of the Royal Society of London A: Mathematical, Physical and Engineering Sciences 459 (2034), The Royal Society, 2003.

[44] M. Lindauer, *Schwarmbienen auf wohnungssuche*, Zeitschrift für Vergleichende Physiologie, 37.4 (1955), pp. 263–324.
Honeybee Ecology: a Study of Adaptation in Social Life, Princeton Univresity Press, Princeton, 1985.

[45] D. Ruelle. *Statistical mechanics: Rigorous results*. W. A. Benjamin, Inc., New York-Amsterdam, (1969).

[46] K. M. Schultz, K. M. Passino, and T. D. Seeley, *The mechanism of flight guidance in honeybee swarms: subtle guides or streaker bees?*, Journal of Experimental Biology 211 (2008), pp. 3287–3295.

[47] M. Scianna and L. Preziosi, *Multiscale developments of the cellular Potts model*, Multiscale Model. Simul. 10 (2012), pp. 342–382.

[48] T. D. Seeley, *Honeybee democracy*, Princeton Univresity Press, Princeton, 2010.

[49] T. D. Seeley, *Honeybee Ecology: a Study of Adaptation in Social Life*, Princeton Univresity Press, Princeton, 1985.

[50] T. D. Seeley, R. A. Morse, and P. K. Visscher, *The natural history of the flight of honey bee swarms*, Psyche, 86 (1979), pp. 103–113.

[51] T. D. Seeley and P. K. Visscher, *Coordinating a group departure: who produces the piping signals on honeybee swarms?*, Behav. Ecol. Sociobiol. 61 (2007), pp. 1615–1621.

[52] T. D. Seeley and S. C. Buhrman, *Group decision making in swarms of honey bees*, Behav. Ecol. Sociobiol. 45 (1999), pp. 19–31.

[53] R. Seidl and W. Kaiser, *Visual field size, binocular domain and the ommatidial array of the compound eyes in worker honey bees*, Journal of comparative physiology 143 (1981), pp. 17–26.

[54] D. J. T. Sumpter, *Collective animal behavior*, Princeton University Press, Princeton, 2010.

[55] J. Toner and Y. Tu, *Long-range order in a two-dimensional dynamical xy model: How birds fly together*, Phys. Rev. Lett. 75 (1995), pp. 4326–4329.

[56] C. M. Topaz and A. L. Bertozzi, *Swarming patterns in a two-dimensional kinematic model for biological groups*, SIAM J. Appl. Math. 65 (2004), pp. 152–174.

[57] C. M. Topaz, A. L. Bertozzi, and M. A. Lewis, *A nonlocal continuum model for biological aggregation*, Bull. Math. Biol. 68 (2006), pp. 1601–1623.

5. Appendix A. Parameter estimate

The proposed approach is intrinsically multiparametric. In particular, the model coefficients can be classified in two groups: those that have a direct and measurable biological meaning (e.g., speed values) and those that are more technical, i.e., that only subsume experimental dynamics, such as the interaction coefficients. We indeed derived a composite parameter setting, obtained by observations and data present both in the experimental and in the theoretical literature and, when necessary, by preliminary numerical realizations.

First, the half visual angle θ_{vis}, which symmetrically extends from the individual gazing direction, was taken equal to $156.5°$, according to the biological measures presented in [53]. We here remark that a visual field determined by such an angle θ_{vis} (i.e., $< 180°$) introduces anisotropy in the behavior of bees although, with respect to most animal species, they are characterized by a substantially limited blind area behind them. As far as we know, in the experimental literature there was instead no study that explicitly defined the depth of the bee visual field. We therefore opted to set d_{vis}=20 m, which is a value that allows each insect to perceive the presence of all groupmates when the swarm is sufficiently compact and not dispersed. The proposed estimate took also into account the domain characteristic dimensions, such as the distance of the nest from the initial position of the insect population: in this respect, d_{vis} was set small enough to avoid that the target destination falls within the visual field of the uniformed individuals at the beginning of the observation time.

In our model two characteristic bee speed values are taken into account. The maximal admissible velocity $v_{\max}$, introduced in Eq. (7) was set equal to 9.4 m/s in accordance with [48]. The mean speed of the uninformed insects, defined in Eq. (16), was instead fixed equal to 6.7 m/s, again coherently with the experimental literature [1]. We here underline that $v_{\max}$ is also used in the case of the fast fly of the streaker bees towards the nest, whereas v_{mean} for the slower backward movement of the passive leader towards the trailing edge of the swarm. The difference between the speed of streakers and of the uninformed individuals has been empirically demonstrated and is at the basis of the rejection of the *subtle* flight alignment hypothesis [48].

All bees, regardless of their status, are characterized by repulsive/attractive interactions. According to the measure reported in [48], the insects tend to preserve a minimal mutual distance, here denoted by d_{avoid}, equal to 0.3 m. The extension of the alignment region d_{align} was taken equal to 2 m. Since this value can not be empirically measured, we obtained its estimate referring to the modelling literature. The ratio $d_{\mathrm{avoid}}/d_{\mathrm{align}}$ used in this work falls in fact in the middle of the range of analogous quantities tested by Couzin and colleagues [20]. A $d_{\mathrm{group}} = d_{\mathrm{vis}}$ was instead set since we have assumed that each insect aims to maintain a connection with all individuals within its visual region.

As already commented in the text, from a mathematical point of view, f_{avoid} (with units m^2/s) gives the slope of the hyperbolic repulsive kernel h^{avoid}, whereas f_{group} (with units m/s) establishes the maximum of the parabolic-type attraction behavior of bees, described by function h^{group}. Both positive parameters indeed do not have a clear and direct experimental counterpart and therefore their estimate was

not straightforward. However, a numerical study, supported by selected empirical evidences, facilitated in this respect. In particular, we first took into account the following considerations: (i) upon attrative/repulsive stimuli only (in the absence of directional, alignment, and random dynamics), the computational swarm has to stabilize in a realistic crystalline configuration, characterized by optimal interparticle spacing $\approx d_{\text{avoid}}$ (i.e., we have to avoid unrealistical situations such as the collapse or the explosion of the insect cloud); (ii) the specific flight of the informed bees has not to be affected by other velocity contributions, in the case of both assumptions L1 and L2.

To account for observation (i), we ran a series of numerical realizations varying the interaction parameters f_{avoid} and f_{group} in the case of a swarm formed by $N = 500$ bees (480 of them with a follower role and the remaining 20 with an initial streaker status), which were assumed to be subject only to repulsive/attractive stimuli, i.e.,

$$\mathbf{v}_i(t) = \mathbf{v}_i^{\text{avoid}}(t) + \mathbf{v}_i^{\text{group}}(t), \tag{27}$$

for all $i = 1, ..., N$, where the interaction velocity components were defined as in Eqs. (11)-(12). Given the same domain Ω and initial conditions described in Section 3.1, the obtained dynamics were then classified according to the following asymptotic quantities:

$$d_{\min} = \min_{\substack{i,j=1,...,N \\ i \neq j}} |\mathbf{x}_i(t_{\text{f}}) - \mathbf{x}_j(t_{\text{f}})|; \tag{28}$$

$$d_{\max} = \max_{\substack{i,j=1,...,N \\ i \neq j}} |\mathbf{x}_i(t_{\text{f}}) - \mathbf{x}_j(t_{\text{f}})|, \tag{29}$$

being t_{f} an observation time sufficiently large to allow the insect cloud to reach a stable equilibrium configuration. The measures introduced in (28)-(29) have clear empirical meanings: $d_{\min}$ is in fact the minimal interparticle distance, whereas $d_{\max}$ defines the extension of the overall swarm. As shown by the representative cases reported in Fig. 13, almost all pairs of coefficients $(f_{\text{avoid}}, f_{\text{group}})$ such that $f_{\text{avoid}}/f_{\text{group}} \geq 10^6$ resulted in realistic swarm pattern, as $d_{\min}$ was very close to the experimentally measured bee comfort space d_{avoid}. In these cases, also the swarm overall diameter $d_{\max}$ was consistent with the empirical observations relative to the spatial density of bees [48]. On the opposite, if $f_{\text{avoid}}/f_{\text{group}} < 10^6$ the insects were observed to stabilize unrealistically close one to another, as $d_{\min} \ll d_{\text{avoid}}$. Such simulation outcomes were indeed able to give a first restriction of the possible variations of the interaction coefficients f_{avoid} and f_{group}. Interestingly, the resulting permitted interaction parameters fall within the H-stability region [2] of the space of interaction parameters $(f_{\text{avoid}}, f_{\text{group}})$ that would characterize pairs of attractive/repulsive interaction kernels analogous to h^{avoid} and h^{group}, with the same coefficients d_{avoid} and d_{group}, if we neglected the asymmetry introduced by the anisotropic visual region of bees (cf. Hypothesis 3 in [6] is not satisfied in our case). In fact, referring to the series of works by Carrillo and colleagues [6–11] (in particular, [11] deals with particle-based models of swarming), and to the calculations proposed in Section 3.2 in [3], we have that the H-stability region for the swarm of our interest in the case of fully isotropic hypotheses (i.e., if the bees had a

---

[2]From statistical mechanics [45], a system of mutual interacting particles is said H-stable if, for any arbitrarily large number of agents, the microscopic agents will not collapse onto themselves and a typical distance between individuals will be well defined.

round visual field) would be given by the following parametric relation:

$$\frac{f_{\text{avoid}}}{f_{\text{group}}} > \frac{2(d_{\text{group}} - d_{\text{avoid}})}{5(d_{\text{avoid}})^2}\left(3(d_{\text{avoid}})^2 + 4d_{\text{group}}d_{\text{avoid}} + 3(d_{\text{group}})^2\right) = 1.0719164 \cdot 10^5,$$
(30)

which is indicated by the grey-shadowed area in Fig. 13 that contains the couples of permitted parameters found by the above numerical investigation. However, despite the consistency between these analytical results and the obtained computational outcomes, it is useful to underline that a theoretical analysis of the H-stability properties of an agent-based system in the case of asymmetric attractive/reulsive kernels is far to be provided and therefore would require further investigations.

Having reduced the range of values of the interaction parameters, we then used the above-cited observation (ii) to have a further estimate. In this respect, we varied the coefficients f_{avoid} and f_{group} in the case of a simulation setting involving a swarm formed again by 480 follower individuals and 20 streaker bees. The insect population, placed in the open-space domain Ω with initial conditions defined again as in Section 3.1, was assumed to behave according to the following rules:

$$\begin{aligned}
\mathbf{v}_i(t) &= \mathbf{v}_i^{\text{avoid}}(t) + \mathbf{v}_i^{\text{group}}(t), \quad \text{if } i : s_i(t) = \text{U}; \\
\mathbf{v}_i(t) &= \mathbf{v}_i^{\text{avoid}}(t) + \mathbf{v}_i^{\text{group}}(t) + \mathbf{v}_i^{\text{streak}}(t), \quad \text{if } i : s_i(t) = \text{S}; \\
\mathbf{v}_i(t) &= \mathbf{v}_i^{\text{avoid}}(t) + \mathbf{v}_i^{\text{group}}(t) + \mathbf{v}_i^{\text{passive}}(t), \quad \text{if } i : s_i(t) = \text{P},
\end{aligned}$$
(31)

for $i = 1, ..., 500$, being the velocity contributions defined exactly as in Section 2 (in particular $\mathbf{v}_i^{\text{passive}}$ was set to take the form either of Eq. (23) or of Eq. (24)). With respect to the complete model, we indeed neglected alignment mechanisms and random contributions. Our choice was justified by the fact that the aim of the study was to find the values of the attraction/repulsion parameters that did not affect the characteristic motion of the informed bees, under the assumptions L1 and L2. As summarized in Figs. 14 and 15, we observed that, in both cases, too large values of f_{group} disrupted the hypothesized flight of the informed bees, regardless of the value given to f_{avoid}. In more details, the group of following bees constantly stabilized into a crystalline configuration but, for $f_{\text{group}} > 10^{-3}$, the following dynamics arose:

- in the case of assumption L1, the scout individuals were not able to reach any edge of the fixed cloud (see the bottom-right panel of Fig. 14);
- in the case of assumption L2, the informed insects were not able to rest at the leading front of the population (where they had to remain since the follower bees had not allowed to have a directional movement and therefore to pass the scouts), as reproduced in the bottom-right panel of Fig. 15.

The underlying rationale involves two competing mechanisms: on one hand, a too large attraction strength f_{group} makes the group of follower individuals almost a rigid disk which is difficult to be flown across; on the other hand, it causes the scout bees to perform an abnormal movement.

Within the remaining set of permitted interaction parameter values, we finally opted to fix $f_{\text{avoid}} = 1 \text{ m}^2/\text{s}$, i.e., we opted for a classical equilateral hyperbolic repulsive kernel as done, for instance, by Kolokolnikov and Chen in the already cited work [12] dealing with predator-prey swarming dynamics. An $f_{\text{group}} = 10^{-6} \text{ m/s}$ was consequently set to avoid further increments in the difference between the order of magnitude of the two parameters.

As seen, a repulsive velocity component from the domain boundary, given by a

negative exponential function, has been set for each bee. In this respect, the insects perceive and react to the presence of the boundaries from a distance of d_{boundary}, whereas a_{boundary} and b_{boundary} determine the exact form of $\mathbf{v}_i^{\text{boundary}}$. In the absence of pertinent experimental measurements, a reasonable estimate of such triplet of coefficients was obtained with a series of preliminary simulations, i.e., in order to avoid unrealistic dynamics such as swarm collapse at the domain boundary or deflection from the optimal flight trajectory at too large distances from the domain edge. In particular, the found values of a_{boundary} and b_{boundary} are analogous to their counterpart employed in a particle model reproducing pedestrian behavior [17]. For the sake of completeness, we illustrate in Fig. 16 some pathological system evolutions in the case of rejected sets of values of d_{boundary}, a_{boundary} and b_{boundary}.

Finally, the modulus of the random velocity vectors falls within the range $[0, v_{\text{mean}}/10]$: in particular, we set such an upper threshold to avoid unrealistically large fluctuations in bee flight, taking also advantage of the study and relative observations performed in [3].

24

Table 1. Model parameters.

Parameter	Description	Value	Reference
d_{vis}	depth of visual field	20 m	biological considerations
θ_{vis}	half visual angle	156.5 degree	[53]
v_{mean}	mean velocity of uninformed bees	6.7 m/s	[1]
v_{max}	bee maximal admissible speed	9.4 m/s	[48]
d_{avoid}	extension of the avoidance region	0.3 m	[48]
d_{align}	extension of the alignment region	2 m	coherent with [19]
d_{group}	extension of the attractive region	20 m	biological considerations
f_{avoid}	avoidance coefficient	1 m^2/s	parametric analysis (cf. Appendix)
f_{group}	attraction coefficient	10^{-6} m/s	parametric analysis (cf. Appendix)
d_{boundary}	extension of the repulsion region from boundary	4.0 m	parametric analysis (cf. Appendix)
a_{boundary}	coefficient of the boundary repulsive velocity	0.18 m/s	parametric analysis (cf. Appendix)
b_{boundary}	coefficient of the boundary repulsive velocity	1.0 m	parametric analysis (cf. Appendix)

Figure 1. (a) The virtual population of bees is modeled in a two-dimensional domain $\Omega \subset \mathbb{R}^2$, i.e., we are taking into account a planar section of a typical swarm. The aim of the insect population is to reach a new nest, which is constituted by a subregion of the domain boundary, hereafter denoted by $\partial\Omega_{\text{nest}}$ ($\subset \partial\Omega$). The domain may represent a large open-space or it may account for environmental elements, such as trees or buildings. (b) The bees within the swarm can have the following roles: U ("uninformed"), S ("streaker"), or P ("passive leader"). An uninformed bee does not change its status, i.e., it is not able to become a scout. Status transitions instead occur within the set of informed insects. More specifically, they are set to have a streaker role while flying towards the nest: in this respect, once reached the front edge of the cloud, they are assigned a passive leader role and turn direction of flight (in the case of hypothesis L1) or stop waiting for the passage of the rest of the insect cloud (in the case of hypothesis L2). Eventually, when a passive leader finds itself at the trailing edge of the swarm, it acquires again a streaker status and move towards the target destination as well.

Figure 2. For each generic insect i, we define a visual region $\Omega_i^{\mathrm{vis}}(t)$. It is a round section determined by the visual depth d_{vis} and the half visual angle θ_{vis}, which symmetrically extends from the gazing direction of bee i, defined by the unit vector $\mathbf{g}_i(t)$ (which, for the sake of simplicity, will be constantly aligned to the velocity $\mathbf{v}_i(t)$). The inclusion of an anisotropic visual field implies that each bee is not able to see and therefore to interact with the entire set of their groupmates (see, for instance, the individual k and h). For representative purposes, hereafter the virtual bees will be indicated by rigid disks centered at their actual position.

Figure 3. (a) Representation of the spatial extension of three interaction regions. The repulsive and attractive sets of the i-th bee, i.e., $\mathcal{N}_i^{\mathrm{avoid}}$ and $\mathcal{N}_i^{\mathrm{group}}$, are in fact given by the insects that i sees and whose distance falls in the ranges $(0, d_{\mathrm{avoid}}]$ and $(d_{\mathrm{avoid}}, d_{\mathrm{group}}]$, respectively. Finally, alternative assumptions are set for the flight synchronization mechanism of uninformed bees. However, in all cases, the insects taken into account by the i-th follower individual have to locate within a distance of $d_{\mathrm{align}} \in (d_{\mathrm{avoid}}, d_{\mathrm{group}})$. (b-c) Plots of the pairwise attractive/repulsive interaction kernels h^{avoid} and h^{group} defined in Eqs. (11) and (12), respectively.

28

Figure 4. The sets of simulations proposed in Section 3.1 are employed in a rectangular $[0, 200] \times [0, 200]$ m^2 domain Ω, where the target destination is constituted by the boundary segment $\partial\Omega_{\text{nest}} = 200 \times [95, 105]$ (indicated by the green line). The swarm is initially arranged in an almost round area centered at (110 m, 100 m) of radius equal to $r_0 = 4$ m, where the positions of the insects are randomly assigned. In particular, we account for $N = 500$ bees, with 480 follower individuals and 20 scouts. All the informed bees are initially assigned a streaker status. For representative purposes, the virtual insects will be hereafter indicated by rigid disks centered at their actual position. More specifically, we will use yellow circles for uninformed individuals, red circles for streaker scouts and blue circles for passive leader scouts.

29

Figure 5. (a) Plot of E_{swarm}, defined in Eq. (25), in the case of 10 independent numerical realizations for each combination of bee behavioral assumptions. It is worth to notice that, in all cases, the swarm undergoes a productive movement, in terms of center of mass displacement. For the sake of completeness, in the inset graph, we represent the evolution in time of the distance of the center of mass of the insect cloud from the nest. (b) Plot of C_{swarm}, defined in Eq. (26), in the case of 10 independent realizations for each combination of bee behavioral assumptions. A consistent (i.e., in all realizations) absence of bee dispersion is only obtained in the case of hypotheses (A3, L1), (A3, L2) and (A4, L2).

30

Figure 6. Representative evolutions of the bee population in the case of combinations between the hypothesis L1 (relative to the behavior of the passive leader scouts) and the alternative assumptions on the alignment mechanism of the follower insects. It is possible to notice that, in all cases, the swarm reaches the target destination, but only for the pair (A3, L1) without bee dispersion. We recall that yellow disks represent follower bees, red circles represent streakers, and blue disks represent passive leaders. For each scout individual, we finally indicate by a colored arrow its velocity.
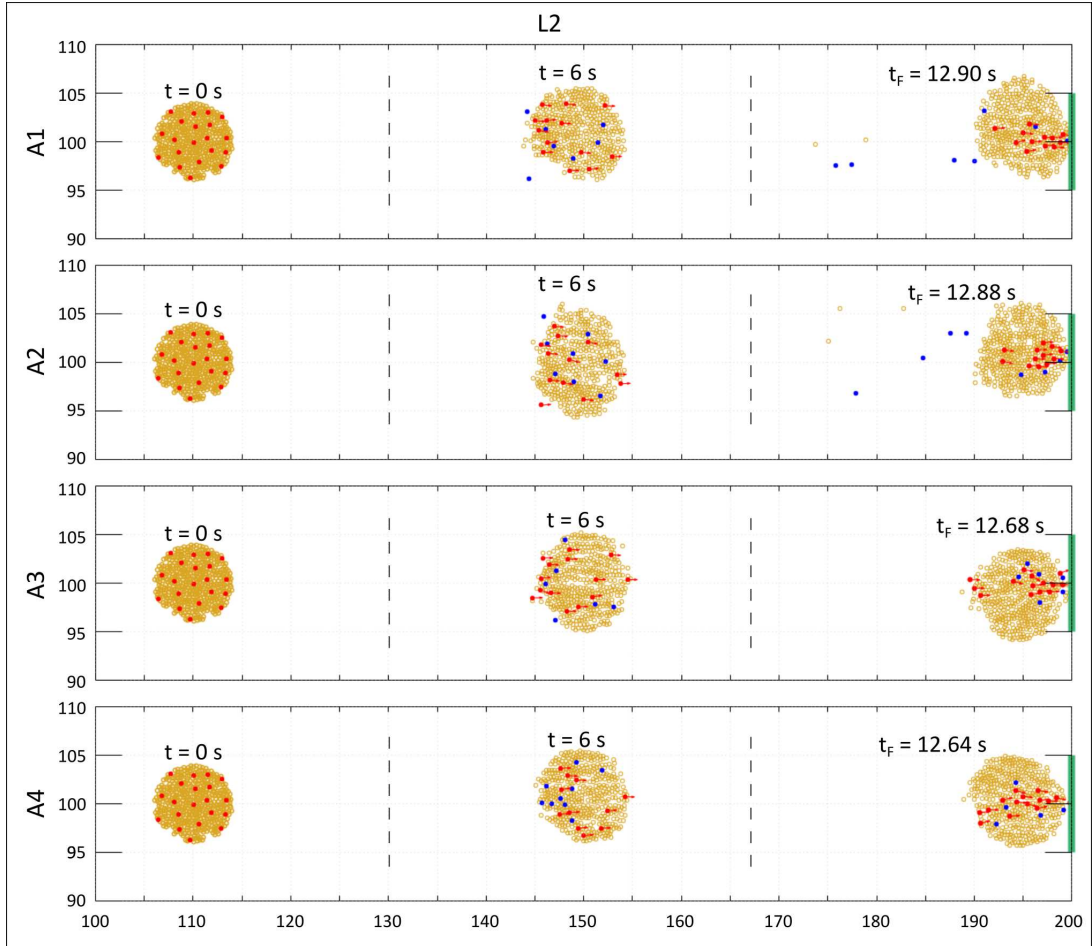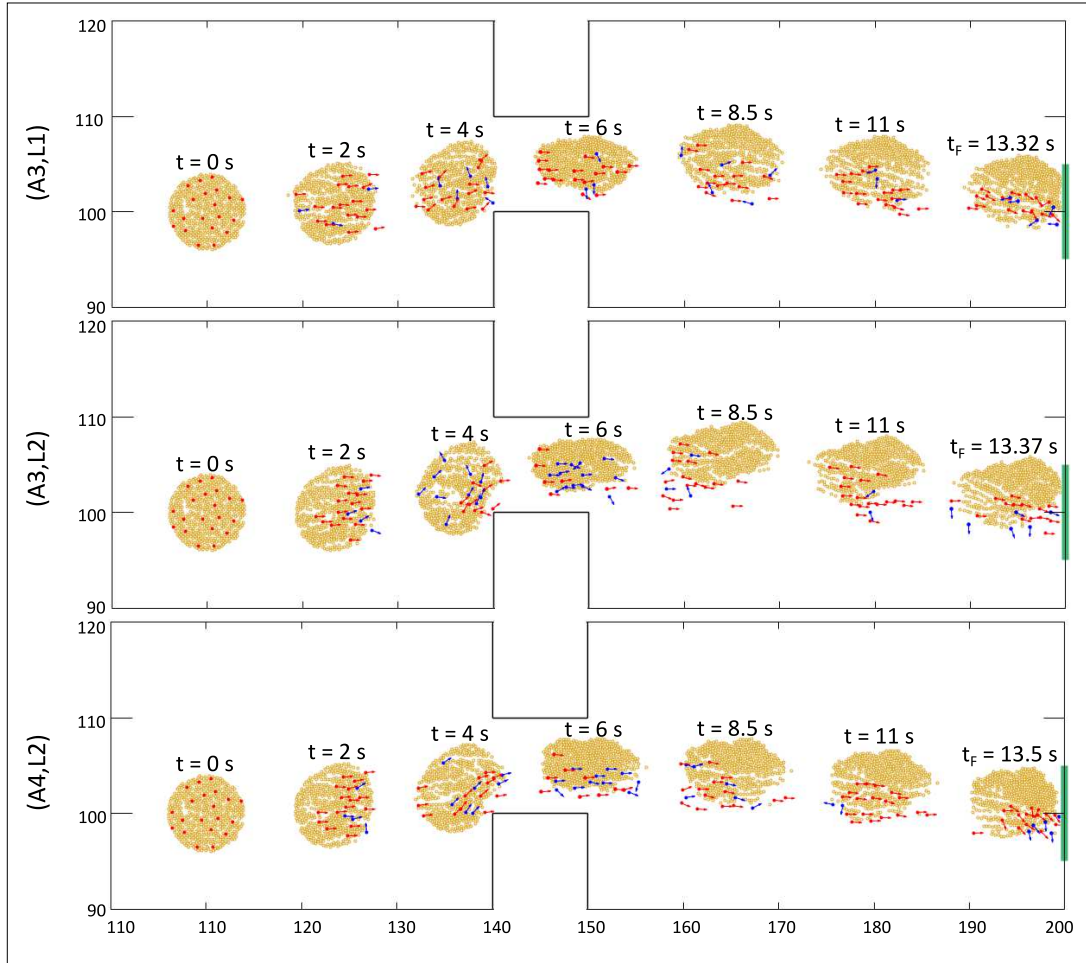
Figure 7. Representative evolutions of the bee population in the case of combinations between the hypothesis L2 (relative to the behavior of the passive leader scouts) and the alternative assumptions on the alignment mechanism of the follower insects. It is possible to notice that, in all cases, the swarm reaches the target destination, bee dispersion is not observed for the pairs (A3, L2) and (A4, L2). We recall that yellow disks represent follower bees, red circles represent streakers, and blue disks represent passive leaders. For each scout individual, we finally indicate by a colored arrow its velocity.
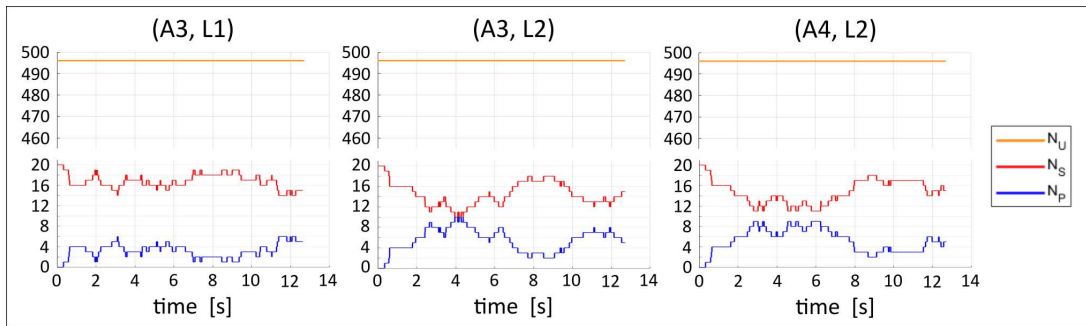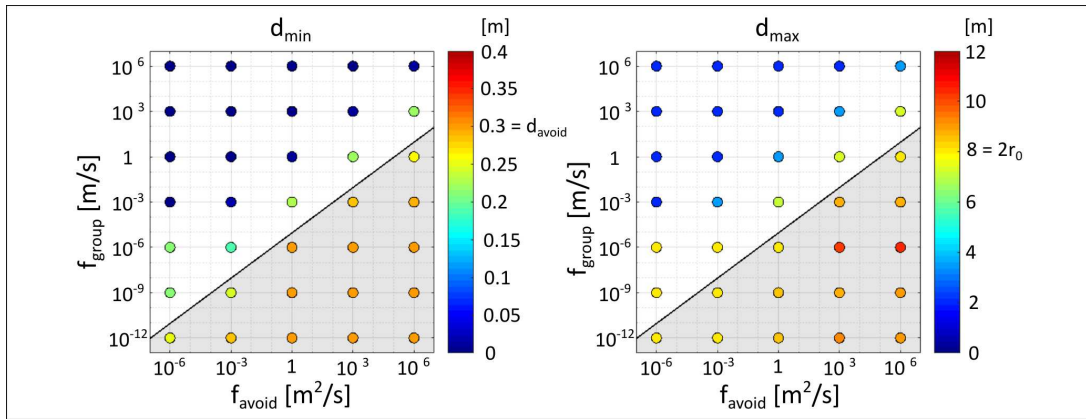
Figure 8. Evolution in time of the number of bees belonging to each subpopulation in the case of hypothesis combinations resulting in directionally productive and collective swarming. For clarity purposes, we plot the outcomes of a single numerical realization for each setting, since we do not observe large variances in the case of multiple independent simulations.
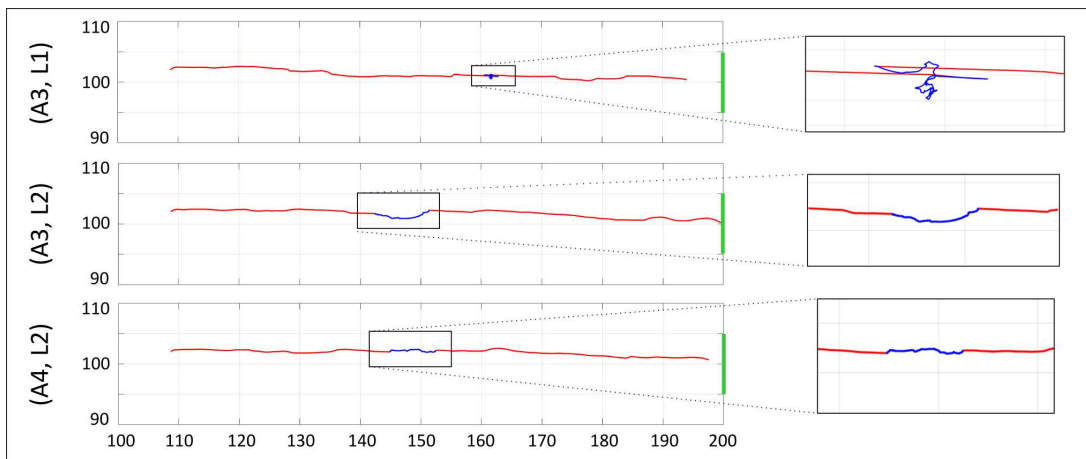
Figure 9. Representative trajectories of scout bees during swarming, in the case of the three combinations of behavioral assumptions resulting in a directionally productive and collective insect flight.
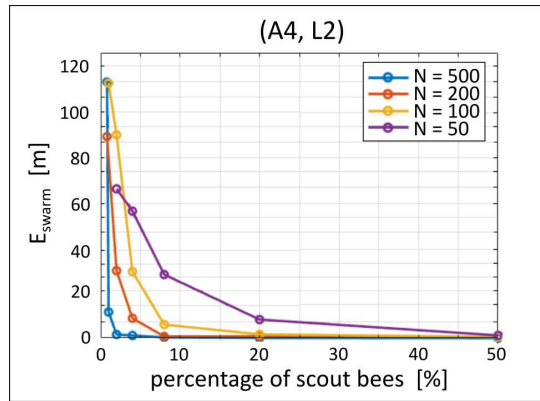
Figure 10. Relationships between the directional efficiency of swarm flight (in terms of E_{swarm}, defined in Eq. (25)) and the percentage of informed bees, in the case of different sizes of the colony (i.e., of overall number of components N). To avoid redundancy, we plot the outcomes obtained from a single realization in the case of coupled hypotheses (A4, L2): however, these results have been obtained also with assumptions (A3, L1) and (A4, L1) and are robust in the case of independent simulations.
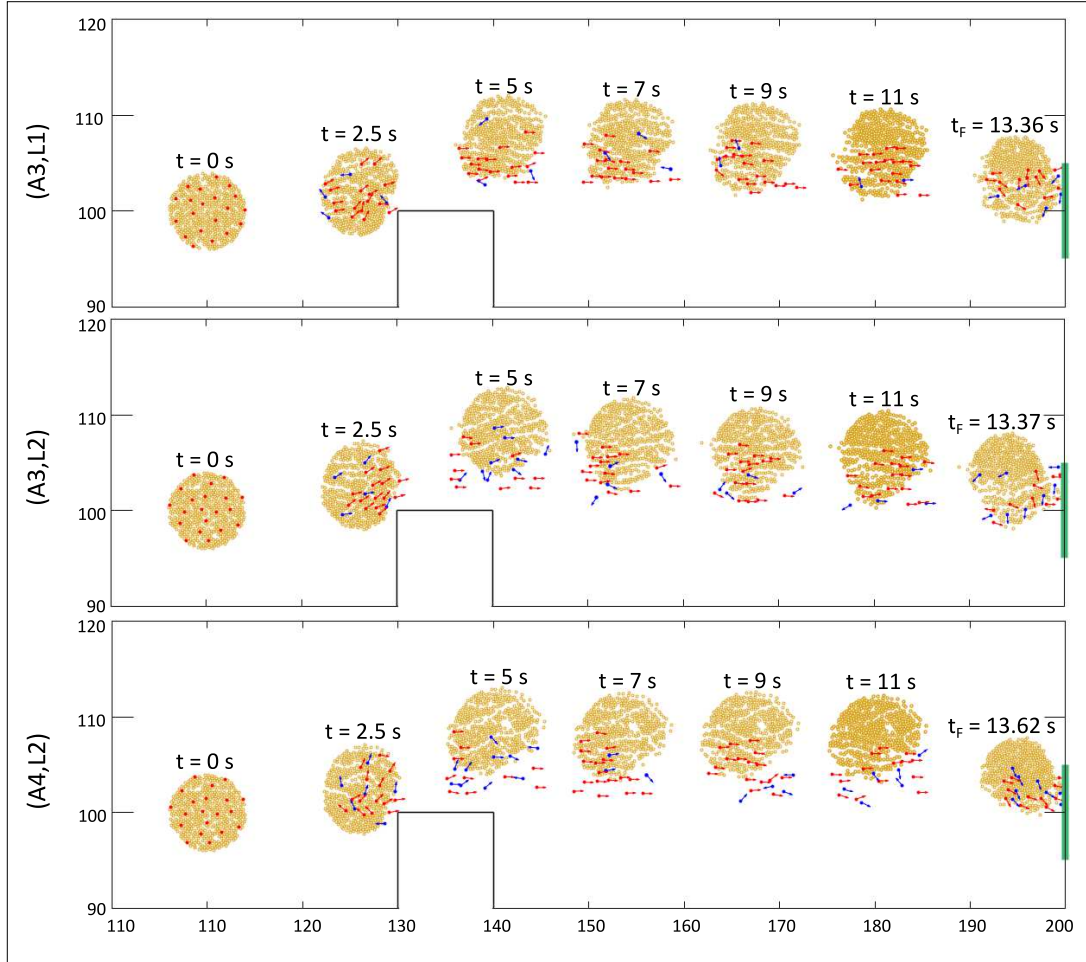
Figure 11. Bee swarming in the case of more complex environments. Representative evolutions of the bee population placed within a domain characterized by a square obstacle between its initial position and the new nest, whose center is located at the same y-coordinate of the initial center of mass of the insect cloud, in the case of the sets of plausible behavioral assumptions (A3, L1), (A3, L2), and (A4, L2). The insect population is assumed to be composed of $N = 500$ individuals, which are initially subdivided into 480 uninformed insects and 20 streakers. The initial configuration of the swarm consists of a circle of radius $r_0 = 4$ m with bee position and gazing direction randomly assigned. It is possible to observe that the swarm autonomously deflects its motion and undergoes morphological reorganization in order to pass the structural element and compactly reach the target destination. We recall that yellow disks represent follower bees, red circles represent streakers, and blue disks represent passive leaders. For each scout individual, we finally indicate by a colored arrow its velocity.

Figure 12. Bee swarming in the case of more complex environments. Representative evolutions of the bee population placed within a domain with a bottleneck between its initial position and the new nest, whose center is located at the same y-coordinate of the initial center of mass of the insect cloud, in the case of the sets of plausible behavioral assumptions (A3, L1), (A3, L2), and (A4, L2). The insect population is assumed to be composed of $N = 500$ individuals, which are initially subdivided into 480 uninformed insects and 20 streakers. The initial configuration of the swarm consists of a circle of radius $r_0 = 4$ m with bee position and gazing direction randomly assigned. It is possible to observe that the swarm squeezes to pass through the structural element. We recall that yellow disks represent follower bees, red circles represent streakers, and blue disks represent passive leaders. For each scout individual, we finally indicate by a colored arrow its velocity.

37

Figure 13. Dependence of the stable configuration of the bee cloud, subjected only to attractive and repulsive dynamics, upon variations in the values of the interaction parameters f_{avoid} and f_{group}. The quantities d_{min} and d_{max} represent the minimal interagent distance and the overall diameter of the swarm at a observation time t_{f} sufficiently large to have a stabilization of the system, as defined in Eqs. (28) and (29), respectively. The grey area in each panel indicates the H-stability region that one would have in the case of the same interaction kernels by assuming a isotropic visual region of bees.

Figure 14. Dependence of the dynamics of the informed bees upon variations in the values of the interaction parameters f_{avoid} and f_{group}, in the case of assumption L1. As it is possible to observe the hypothesized "back-and-forth" flight can be obtained only for $f_{\text{group}} < 10^{-3}$, regardless of the values of coefficient f_{avoid} (provided that the pair (f_{avoid}, f_{group}) leads to crystalline equilibrium configurations upon attractive/repulsive interactions only). Too large values of f_{group} in fact result in a disrupted behavior of the informed insects, which remain stuck within the bee cloud (represented by the yellow shadow), as reproduced in the corresponding representative bottom panel.

Figure 15. Dependence of the dynamics of the informed bees upon variations in the values of the interaction parameters f_{avoid} and f_{group}, in the case of assumption L2. As it is possible to observe the hypothesized "go-and-stop" flight can be obtained only for $f_{group} < 10^{-3}$, regardless of the values of coefficient f_{avoid} (provided that the pair (f_{avoid}, f_{group}) leads to crystalline equilibrium configurations upon attractive/repulsive interactions only). Too large values of f_{group} in fact result in a disrupted behavior of the informed insects, which are not able to stop at the leading edge of the bee cloud (represented by the yellow shadow) being dragged within the population, as reproduced in the corresponding representative bottom panel.

Figure 16. Unrealistic bee swarming in the cases of representative rejected sets of parameters relative to the velocity component $\mathbf{v}^{\text{boundary}}$. (a) The bee swarm collapses on the domain structural element being unable to react to its presence. This phenomenology can be obtained, for instance, with a too low value of d_{boundary} and a too high value of b_{boundary}. (b) The insect population deforms at an implausibly high distance from the obstacle. This system behavior is instead the result of too high values of d_{boundary} and a_{boundary}.

Figure 1: (a) The virtual population of bees is modeled in a two-dimensional domain $\Omega \subset \mathbb{R}^2$, i.e., we are taking into account a planar section of a typical swarm. The aim of the insect population is to reach a new nest, which is constituted by a subregion of the domain boundary, hereafter denoted by $\partial\Omega_{\text{nest}}$ ($\subset \partial\Omega$). The domain may represent a large open-space or it may account for environmental elements, such as trees or buildings. (b) The bees within the swarm can have the following roles: U ("uninformed"), S ("streaker"), or P ("passive leader"). An uninformed bee does not change its status, i.e., it is not able to become a scout. Status transitions instead occur within the set of informed insects. More specifically, they are set to have a streaker role while flying towards the nest: in this respect, once reached the front edge of the cloud, they are assigned a passive leader role and turn direction of flight (in the case of hypothesis L1) or stop waiting for the passage of the rest of the insect cloud (in the case of hypothesis L2). Eventually, when a passive leader finds itself at the trailing edge of the swarm, it acquires again a streaker status and move towards the target destination as well.

Figure 2: For each generic insect i, we define a visual region $\Omega_i^{\text{vis}}(t)$. It is a round section determined by the visual depth d_{vis} and the half visual angle θ_{vis}, which symmetrically extends from the gazing direction of bee i, defined by the unit vector $\mathbf{g}_i(t)$ (which, for the sake of simplicity, will be constantly aligned to the velocity $\mathbf{v}_i(t)$). The inclusion of an anisotropic visual field implies that each bee is not able to see and therefore to interact with the entire set of their groupmates (see, for instance, the individual k and h). For representative purposes, hereafter the virtual bees will be indicated by rigid disks centered at their actual position.

Figure 3: (a) Representation of the spatial extension of three interaction regions. The repulsive and attractive sets of the i-th bee, i.e., $\mathcal{N}_i^{\text{avoid}}$ and $\mathcal{N}_i^{\text{group}}$, are in fact given by the insects that i sees and whose distance falls in the ranges $(0, d_{\text{avoid}}]$ and $(d_{\text{avoid}}, d_{\text{group}}]$, respectively. Finally, alternative assumptions are set for the flight synchronization mechanism of uninformed bees. However, in all cases, the insects taken into account by the i-th follower individual have to locate within a distance of $d_{\text{align}} \in (d_{\text{avoid}}, d_{\text{group}})$. (b-c) Plots of the pairwise attractive/repulsive interaction kernels h^{avoid} and h^{group} defined in Eqs. (11) and (12), respectively.

Figure 4: The sets of simulations proposed in Section 3.1 are employed in a rectangular $[0, 200] \times [0, 200]$ m^2 domain Ω, where the target destination is constituted by the boundary segment $\partial\Omega_{\text{nest}} = 200 \times [95, 105]$ (indicated by the green line). The swarm is initially arranged in an almost round area centered at (110 m, 100 m) of radius equal to $r_0 = 4$ m, where the positions of the insects are randomly assigned. In particular, we account for $N = 500$ bees, with 480 follower individuals and 20 scouts. All the informed bees are initially assigned a streaker status. For representative purposes, the virtual insects will be hereafter indicated by rigid disks centered at their actual position. More specifically, we will use yellow circles for uninformed individuals, red circles for streaker scouts and blue circles for passive leader scouts.

Figure 5: (a) Plot of E_{swarm}, defined in Eq. (25), in the case of 10 independent numerical realizations for each combination of bee behavioral assumptions. It is worth to notice that, in all cases, the swarm undergoes a productive movement, in terms of center of mass displacement. For the sake of completeness, in the inset graph, we represent the evolution in time of the distance of the center of mass of the insect cloud from the nest. (b) Plot of C_{swarm}, defined in Eq. (26), in the case of 10 independent realizations for each combination of bee behavioral assumptions.

A consistent (i.e., in all realizations) absence of bee dispersion is only obtained in the case of hypotheses (A3, L1), (A3, L2) and (A4, L2).

coordinate of the initial center of mass of the insect cloud, in the case of the sets of plausible behavioral assumptions (A3, L1), (A3, L2), and (A4, L2). The insect population is assumed to be composed of $N = 500$ individuals, which are initially subdivided into 480 uninformed insects and 20 streakers. The initial configuration of the swarm consists of a circle of radius $r_0 = 4$ m with bee position and gazing direction randomly assigned. It is possible to observe that the swarm squeezes to pass through the structural element. We recall that yellow disks represent follower bees, red circles represent streakers, and blue disks represent passive leaders. For each scout individual, we finally indicate by a colored arrow its velocity.

Figure 13: Dependence of the stable configuration of the bee cloud, subjected only to attractive and repulsive dynamics, upon variations in the values of the interaction parameters f_{avoid} and f_{group}. The quantities d_{min} and d_{max} represent the minimal interagent distance and the overall diameter of the swarm at a observation time t_{f} sufficiently large to have a stabilization of the system, as defined in Eqs. (28) and (29), respectively. The grey area in each panel indicates the H-stability region that one would have in the case of the same interaction kernels by assuming a isotropic visual region of bees.

Figure 14: Dependence of the dynamics of the informed bees upon variations in the values of the interaction parameters f_{avoid} and f_{group}, in the case of assumption L1. As it is possible to observe the hypothesized "back-and-forth" flight can be obtained only for $f_{\text{group}} < 10^{-3}$, regardless of the values of coefficient f_{avoid} (provided that the pair (f_{avoid}, f_{group}) leads to crystalline equilibrium configurations upon attractive/repulsive interactions only). Too large values of f_{group} in fact result in a disrupted behavior of the informed insects, which remain stuck within the bee cloud (represented by the yellow shadow), as reproduced in the corresponding representative bottom panel.

Figure 15: Dependence of the dynamics of the informed bees upon variations in the values of the interaction parameters f_{avoid} and f_{group}, in the case of assumption L2. As it is possible to observe the hypothesized "go-and-stop" flight can be obtained only for $f_{\text{group}} < 10^{-3}$, regardless of the values of coefficient f_{avoid} (provided that the pair (f_{avoid}, f_{group}) leads to crystalline equilibrium configurations upon attractive/repulsive interactions only). Too large values of f_{group} in fact result in a disrupted behavior of the informed insects, which are not able to stop at the leading edge of the bee cloud (represented by the yellow shadow) being dragged within the population, as reproduced in the corresponding representative bottom panel.

Figure 16: Unrealistic bee swarming in the cases of representative rejected sets of parameters relative to the velocity component $\mathbf{v}^{\text{boundary}}$. (a) The bee swarm collapse on the domain structural element being unable to react to its presence. This phenomenology can be obtained, for instance, with a too low value of d_{boundary} and a too high value of b_{boundary}. (b) The insect population deforms at an implausibly high distance from the obstacle. This system behavior in instead the results of to high values of d_{boundary} and a_{boundary}.